Highly sensitive coulometric detection of proteins based on metallization

Isa Anshori

February 2018

Highly sensitive coulometric detection of proteins based on metallization

Isa Anshori

Doctoral Program in Nano-Science and Nano-Technology

Submitted to the Graduate School of
Pure and Applied Sciences
in Partial Fulfillment of the Requirements
for the Degree of Doctor of Philosophy in
Engineering

at the
University of Tsukuba

Table of contents

Abstract

Along with the advancement progress of healthcare service, the presence of μTAS (Micro Total Analysis System) becomes significant as a popular analytical tool for the detection of the diseases. Among the successful development of lab-on-chip (LOC), electrochemical-based devices provide a simple approach for direct on-site analysis. Its characteristics for rapid and accurate detection, and low cost fabrication opened up the huge applications in the clinical service. Electrochemical microdevice combined with the gold standard detection of the diseases using enzyme-linked immunosorbent assay (ELISA) has been extensively studied. To improve the performance of previous coulometric microdevice, coupling the coulometry method with metallization shows interesting results (**Ikemoto et al., 2016**). In this system, the redox reactions were located in different chambers on a single electrode. The information of analyte was measured by the amount of the deposited metal. This principle comes from the concept of mixed potential. Mixed potential is the potential observed when several redox reactions proceed simultaneously, and settles at a value at which the sum of the anodic and cathodic currents is zero. Using this technique, the profile of the coulometric charge was changed. The background was increased gradually in much smaller scale than the conventional coulometry. Interestingly, the response charge was increased rapidly and the slope was dropped suddenly in the same level of the background which indicate that the deposited silver on the working electrode was removed completely after the coulometry was conducted. This study focuses on the development and characterization of microdevice based on coulometry coupled with silver metallization for immunoassay purposes. Realization of the LOC device for ELISA which consumed a minute volume or reagents is the main interest of this research project.

Firstly, a coulometric microdevice for protein detection was developed in this study. Coulometry method was selected among other electrochemical methods due to its advantage in analyzing the sample of a minute volume. In this device, reagents of interest were processed in the form of plugs of 1.5 μL. The plug was formed by splitting the solution using air pressure in a T-shape configuration. For the purpose of immunoassay detection, a self-assembled monolayer (SAM) of cysteine was formed on the gold electrode to bind the capture antibodies on it. Complex structure of capture antibodies, antigen, and detection antibodies labeled with enzymes was then formed. The detection method of this device was based on coulometry coupled with silver metallization and the analyte is the enzymatic product of the enzyme and the substrate solution. Information of the concentration of the analyte (hydrogen peroxide) in one flow channel (flow channel A) was transferred into the amount of silver deposited on the other flow channel (flow channel B) through the mixed potential mechanism. Optimization of several parameters for detections of the proteins was conducted. SAM formation for binding the capture antibodies and the improvement of sensitivity through replacing the substrate plug every 30 min were shown. The coulometric charge changes by increasing the time of enzymatic reaction. The estimated LOD for 120 min enzymatic reaction process was 0.4 ng/mL.

In the next step, modification of the coulometric device was conducted to enhance the signal generation through shifting the mixed potential. For this purpose, liquid junction which connected the two flow channels were replaced with the silver wire as a metal junction. Using this configuration, the shifting of mixed potential can be controlled by several ways. The first method is the changing the electrolyte concentration in the electrolyte container of flow channel B. KCl concentrations of 0.01 M, 0.1 M, and 1 M were tested. Using 0.01 M KCl as an electrolyte, the mixed potential was shifted higher. Using low concentration of electrolyte (KCl) in the analyte in flow channel A could shift the mixed potential and increase the current, thus increasing the amount of deposited silver on the working electrode in flow channel B. However, the difference between the potentials of working electrode in flow channel A ($\Delta\varphi_1$) and working electrode in flow channel B ($\Delta\varphi_2$) was small (<100 mV). To obtain more deposited silver under such condition is not possible. Due to this reason, further increasing the amount of deposited silver by using much lower concentration of the electrolyte in the analyte was not preferable. From the second experiment, the mixed potential can be shifted to increase the amount of deposited silver by modifying one end of the metal junction. Nickel or zinc was deposited on one end of the metal junction. Standard electrode potentials of nickel ($E^0 = -0.257$ V) and zinc ($E^0 = -0.7626$ V) are more negative than silver ($E^0 = 0.7991$ V). Replacing the AgCl layer with zinc or nickel increases the oxidation reaction in the electrolyte compartment. Modifying one end of the silver wire with zinc gave a much higher response than with AgCl and nickel. Although the difference between $\Delta\varphi_1$ and $\Delta\varphi_2$ was much increased in the of zinc which gave high output charge, controlling the value of $\Delta\varphi_1$ and $\Delta\varphi_2$ by careful selection of the appropriate metal to be deposited is still impractical and not preferable. In the third experiment, the mixed potential wants to be shifted in the higher current by applying a potential difference between flow channel A with respect to the electrolyte compartment. From this configuration, when the negative potential was applied, the electrons will move on the direction from the Pt working electrode of flow channel A to the Pt working electrode of flow channel B. Thus, the silver deposition on the working electrode in flow channel B can be increased or accumulated. At first, potential from -0.1 V to -0.8 V were tested for deposition of the silver. Potentials lower than -0.6 V have unsaturated coulometric responses. Potential of -0.6 V give the highest output charge than the potential from -0.1 V to -0.5 V. Longer incubation also increased the amount of deposited silver. Detection limit of H_2O_2 of 2.4 nM was achieved using applied potential of -0.6 V for 10 min silver deposition. Such approach gave a simple way to control the amount of deposited silver in a coulometry coupled with silver metallization.

Final part of this study is further optimization of the device from the coulometric microdevice using the liquid junction for improving several parameters related with decreasing the background signal and increasing the response signal and also the modification of the device structure. First modification is the optimization of the blocking condition for the ELISA. Second modification is reducing the plug volume to increase the accumulated product of enzymatic reaction in ELISA. Third modification is removing the auxiliary flow channel connected to flow channel A to minimize the loss of antibodies or proteins during the plug volume measurement. Response signal was improved. Next, structure changing of the Pt electrode in flow channel A from rectangular structure into comb structure was conducted. This result in the reduction of the background

charge. Third modification is the reduction of the number of pinholes and the pinhole diameter in the working electrode in flow channel B. Optimum condition was obtained using the number of pinholes of 2 and the pinhole diameter of 3 μm. Significant reduction of the background with small reduction of the response signal was obtained in this configuration.

Detection of AFP was tested using these optimized conditions and combined with the silver deposition method by applying potential from external voltage source. Silver deposition was conducted by applying potential –0.6 V from the voltage source for 10 min. AFP concentrations from 1 ng/mL to 10 ng/mL were detected. Limit of detection for AFP was 76.7 pg/mL (3σ). Finally, enhancement strategy through redox cycling was tested in this study. For this experiment, the structure of the device was modified to include additional electrode in the sensing area of flow channel A. The enzyme that label to the detection anti-AFP was changed from glucose oxidase to alkaline phosphatase to produce p-aminophenol (PAP); the enzymatic reaction product that can be redox cycled. For the preliminary experiment to check the performance of the device based on redox cycling technique, detection of PAP was conducted. Detection limit of 80 pM was achieved using the device based on redox cycling technique. Next, AFP detection was conducted from 0.1 ng/mL to 1 ng/mL. Detection limit of 19.6 pg/mL (3σ) was obtained. The detection limit was improved 4 times than that when using the metal wire connected with external voltage source. From this study, redox cycling technique has been successfully integrated with the method of coulometry coupled with silver metallization.

Chapter 1 Introduction

1.1 Motivation

Millenium Development Goals (MDGs) from United Nation (UN) gives a framework for speed up the decline of infectious diseases. Numerous successes have been credited such as the decrease of death rates of more than a quarter in the case of malaria infection (**United Nation, 2013**). Despite these positive results, infectious diseases remain one of the most causes of death in developing countries from the diseases such as diarrheal, HIV/AIDS, tuberculosis, and malaria. The threat of pandemics have become a global concern (**Dye, 2014**). Nevertheless, the number of deaths has fallen only slowly with the number estimated to be 13 million in 2050 (**Figure 1A**). The victims of the infectious diseases were mostly the people from low and middle income categories (**Figure 1B**). The only ultimate goal of controlling infectious disease is to achieve total eradication. A good example is found in the eradication of smallpox and there is optimism that such eradication is a reality that can be accomplished (**Nii-Trebi, 2017**). However, development of the effective tools was not easy because of some problems such as antibiotics resistance and the slow progress to find effective vaccines. As one of the important components to control the infectious diseases, continuous surveillance and early detection are very important to intervene. Building up a simple infrastructure to support point-of-care testing (POCT) in a limited environment will massively aid the national healthcare program. The POCT is defined as analytical testing that is performed outside the central laboratory using instruments or devices that can be easily transported to the location of patient (**Holland et al., 2005**). The locations range from small clinic, local emergency laboratory, bedside monitoring to personal self-testing. The market growth and demand for *in vitro* diagnosis (IVD) has approximately reached US$18 billion in 2016 (**St John et al., 2014**). From the data of 2011, 55% of it was used in US, 30% in Europe and 12% in Asia. In the case of POCT of infectious diseases, total diagnostic market was approximately US$7 billion with annual growth rates more than 18%. For life-threatening conditions such as meningitis or malaria where commonly diagnosed presumptively in patients with fever (**Murray et al., 2008**), POCT can quickly produce the data on-site, thus immediate treatments can be conducted in the ideal case (**Price et al., 2001**).

Molecular diagnostics have become the foundation in a modern healthcare. Health monitoring depends on the ability to detect pathogens. Ideal treatments should be started from the clear examination of the sample analysis followed with properly selecting the medication. This approach will eliminate overtreatment and misdiagnosis of potentially fatal infections. Laboratory research also needs the quantification of many targets of biomolecules for other purposes such as drug screening or protein characterization. Although these are only a few examples, development of a sensors for detection and quantification of proteins and small molecules in a sample could give a wide range of applications. In the case of global pandemic diseases such as influenza or HIV, POC diagnosis for protein will help identify disease-causing pathogens, enabling simpler and more efficient treatment, and finally improve the management of the disease control. Highly sensitive diagnostics of the protein could play a key role in surveillance for early detection of sporadic outbreaks.

For such field deployment purpose, the system must be portable, which imply the need of power, weight, and total volume in a small scale. It should ideally be used in a simple way and require minimal reagents or consumable solutions. Immunological assay techniques have become the golden standard for detection method of infectious diseases. However, proper facilities with minimum equipment for conducting immunoassay are mostly unavailable if the locations are far from the big cities. Therefore, there is a growing need to decentralize the practices of molecular diagnostic and perform the analysis in many kind of locations.

This dissertation focuses on the development and characterization of such platform for immunoassay purposes. Electrochemical-based method was selected due to a higher possibility to be adapted in a resource limiting environment.

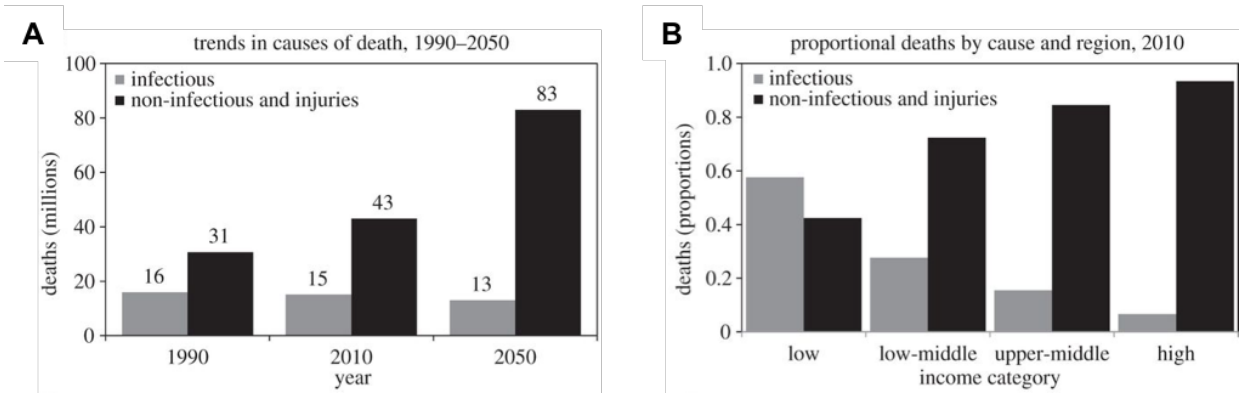

Figure 1.1. Deaths from the infectious and non-infectious diseases worldwide (**Dye et al., 2014**). (A) Past estimation and future prediction of the number of deaths. (B) Proportion of deaths based on income category. Figure was taken from ref. **Dye et al., 2014** published by the Royal Society under the terms of the Creative Commons Attribution License http://creativecommons.org/licenses/by/3.0/, which permits unrestricted use, provided the original author and source are credited.

1.2 Development of POC diagnostic tools using lab-on-a-chip technologies

Lab-on-a-chip (LOC) is a system where necessary components for the biological or chemical analysis could be integrated onto a miniaturized single chip using micro or nanofabrication technology. Integration of multiple functions such as pre-treatment of samples, manipulations of samples and detection of target analyte that may be performed with integrated valves and pumps in a sample can be realized in a single chip. There is a long history of LOC and microfluidic technologies which began from a basic research to the products available today in hospitals or clinics. Some earliest researches on liquid processing with high accuracy and precision were found on the development of gas chromatography and electrophoresis (**Martin et al., 1941; Kunkel et al., 1954; Whitesides, G. M., 2006**). These two projects revolutionized the approach on chemical analysis for analyzing a very small sample with high sensitivity. Within similar period of time, first development of ink-jet printing technology by Siemens marked the first commercial application of

microfluidic devices (**Le et al., 1998**). Demands of high control ability of liquid for advanced chemical analysis and more complex applications lead to the studies of micropump (**Woias et al., 2005**) and microvalves (**Terry et al., 1975; Oh et al., 2006**). A decade later, a general concept of miniaturized total analysis system (μTAS) was introduced (**Manz et al., 1990**) in which sample treatment, separation, and detection have a fundamental aspect. μTAS has the similar term with LOC. This is the renaissance period where the interest of developing a portable sensing device with good selectivity and lifetime arise. Although the earlier reason of device miniaturization was to enhance the device performance for the analysis rather than only made it smaller. It later became a major interest and achieved immediate attention due to the fact that a small size device only requires a small consumption of reagents or samples to be analyzed and the possibility for mass production.

Microfluidics characterized by the method to manipulate fluids in the order of submillimeter scale. The phenomena of the liquid at this scale were different than those dominating the macroscale liquid. For example, surface tension and interfacial tension are dominant at the microscale while the gravity is much dominant at the macroscale. In a microscale, capillary forces also dominant, which allow the liquid to move against the gravity. Pregnancy test and glucometer are based on this phenomenon. Because of the small dimension of the microchannel, the Reynolds number is small (1-100), which gives the characteristics of the flow become laminar and the turbulence not appears. Reynolds number is the ratio of inertial forces to viscous forces and is a convenient parameter for predicting if a flow condition will be laminar or turbulent. The transition to turbulent flow generally occurs in the range of Reynolds number of 2000. Laminar flow provides a means by which molecules can be transported in a relatively predictable manner through microchannels. These phenomena can be utilized for varied tasks, such as passive pumping of the liquid in microchannels (**Walker, G. A., 2002**), analytes filtration (**Berry et al., 2012**), and monodisperse droplets formation (**Anna et al., 2003**).

On the other hand, soft lithography using elastomeric materials was developed for microfluidic applications by the group of Bell Labs (**Aumiller et al., 1974**) and for cell biology applications by Nanba's group (**Masuda et al., 1989**). The techniques were then used by Whitesides's group with polydimethylsiloxane (PDMS) (**Duffy et al., 1998**). Since then, PDMS has become the most widely used elastomeric material due of its useful properties such as biocompatibility, low toxicity, low cost, chemical inertness, mechanical flexibility, transparency, and durability. In addition, fabrication of the PDMS substrate device for designing the microfluidic structure only require few equipments. These properties made PDMS easily adopted in LOC for biomedical research purposes. With the advancement of the technologies, other manufacturing methods such as hot embossing, injection molding, cutting and machining, and 3D printing. Hot embossing uses a heated mold then press against the thermoplastic block, creating an inverted replica (**Becker et al., 2000**). In injection molding, a molten thermoplastic was injected into a closed mold chamber and then solidified by cooling the mold. (**Attia et al., 2009**). Cutting technique using cutter plotter was used to form microchannel (**Bartholomeusz et al., 2005**), and machining technique can create 3D microstructure, although with a large roughness on the surface (**Gujkenberger et al., 2015**). 3D printing is the latest technique that received many attentions because of its possibility to change the current trends in microfabrication. 3D printer offers the capabilities to fabricate a master mold (**Comina et al., 2013**) and even a complete device (**Comina et al.,**

2014). All these fabrication techniques promise the easiness and flexible development of microfluidic device.

LOC technologies give the opportunity of analyzing a minute volume of samples which can be the new standard for rapid test. Portability and accurate diagnosis through carefully processing the reactions involved between receptor and analyte when taking the test are provided in the LOC system. Currently, there are two main interests that drive the research on LOC for healthcare applications: POCT and diagnostics for central laboratory. LOC have a big market in the research of life sciences. Immunoassays procedure, drug screening, and cell studies. Depending on the experiments that were conducted, researchers or technicians may need to change reagents, analytes, and the test procedure frequently. The time spends for obtaining the result can change from seconds, minutes, to hours, which in urgent cases are not preferable. LOC technologies opened

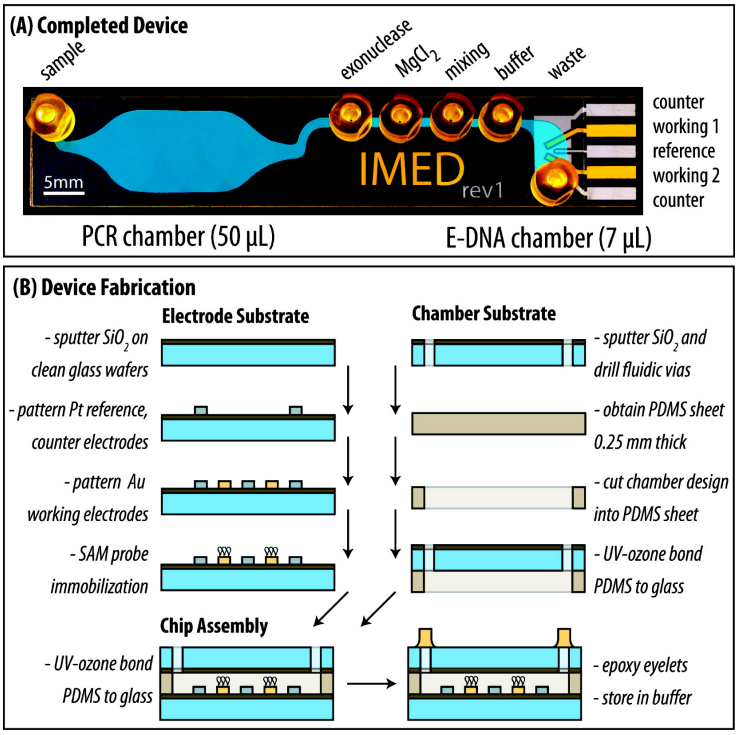

Figure 1.2. Example of the LOC device for DNA sensor (**Ferguson et al., 2009**). (A) Schematic of an integrated microfluidic device along with its components. (B) Fabrication step of the device. Reprinted with permission from ref. **Ferguson et al., 2009**. Copyright 2009 American Chemical Society.

up the ways for automatic analysis of the samples (**Gomez-de Pedro et al., 2017**; **Samiei et al., 2016; Tai et al., 2007**). By this way, the cost of experiment or research could be reduced substantially. Because the necessary sample is reduced, it will also contribute to the amount of waste, which is beneficial for the environment. Because all of the samples are limited in a very small reaction or sensing region, the surface to volume ratio is increased significantly. Other advantages are a good diffusion and attachment of the samples to the sensing area. A minute region also results in a rapid progression of the reactions, thus shortening the

detection time. Owing to such excellent properties that are suitable for on-site detection, the LOC has many advantages when it is adopted in various kind of chemical and biological analysis.

Biosensor is POC diagnostic device that use a biological recognition element such as antibodies, nucleic acids, or aptamers immobilized on the surface of transducer, and connected to the detector. Interaction of the target analyte inside the sample with the transducers are important in biosensor. Detector responses the presence of the target analyte in a sample and record it, providing a relation between the amount of analyte and its physical response signal (optical or electrical signal). Many kinds of samples have regularly been tested in POCT such as body fluids (blood, saliva, urine), protein and antibody. Biological recognition elements, such as antibody for immunoassay, need to be immobilized on the sensing area of the device to act as a receptor and recognize the target inside the sample. Different methods have been tested to immobilize the biological recognition elements such as covalent bonding, entrapment, adsorption, etc. Adsorption and entrapment are categorized as physical immobilization method. They usually conducted on biocompatible materials to prevent the damage of antibodies or antigens. The problems of adsorption method may arise related with the adsorption of non-specific protein, the biomolecules stability, and the possibility of biomolecules desorption because of

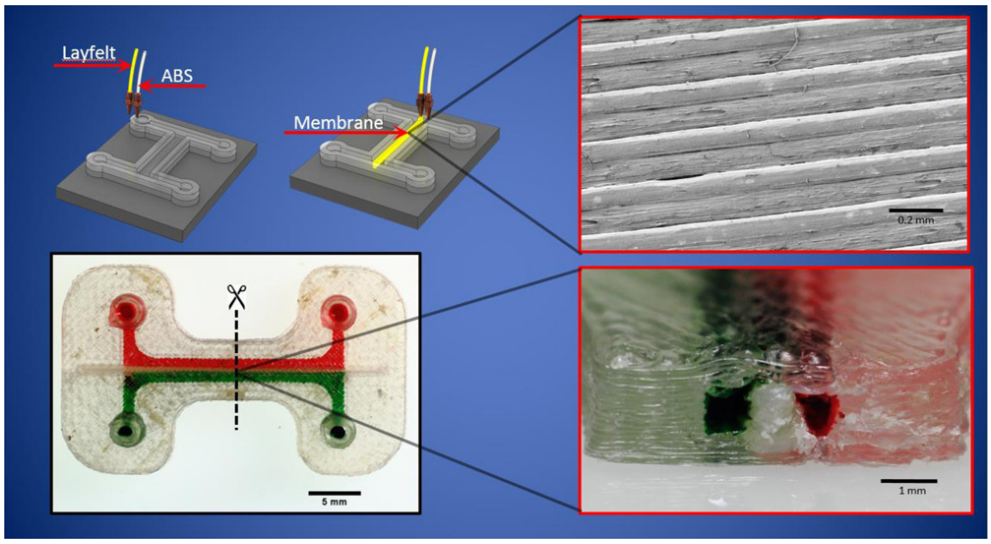

Figure 1.3. Integrated 3D printed chip with membrane layer (**Li et al., 2017**). Reprinted with permission from ref. **Li et al., 2017**. Copyright 2017 American Chemical Society.

physical or chemical change. These problems can be reduce using the entrapment method. However, there is still a problem of unintended blocking of the immunorecognition sites of antibodies or antigens which can reduce the performance of the device.

Chemical immobilization involves surface treatment of the solid support of the transducer to attach antibodies or antigens on it. Covalent bonding immobilization is the most preferable method because of its

stability, thus minimizing the detachment of the biological elements from the support surface (**Datta et al., 2012**). The surface treatments are also critical to repel or block the unwanted bonding to the transducer from non-target analytes contained in the sample. Formation of self-assembled monolayers (SAM) is one of the common strategy to provide a versatile and simple way of surface treatment of the device. SAM molecules

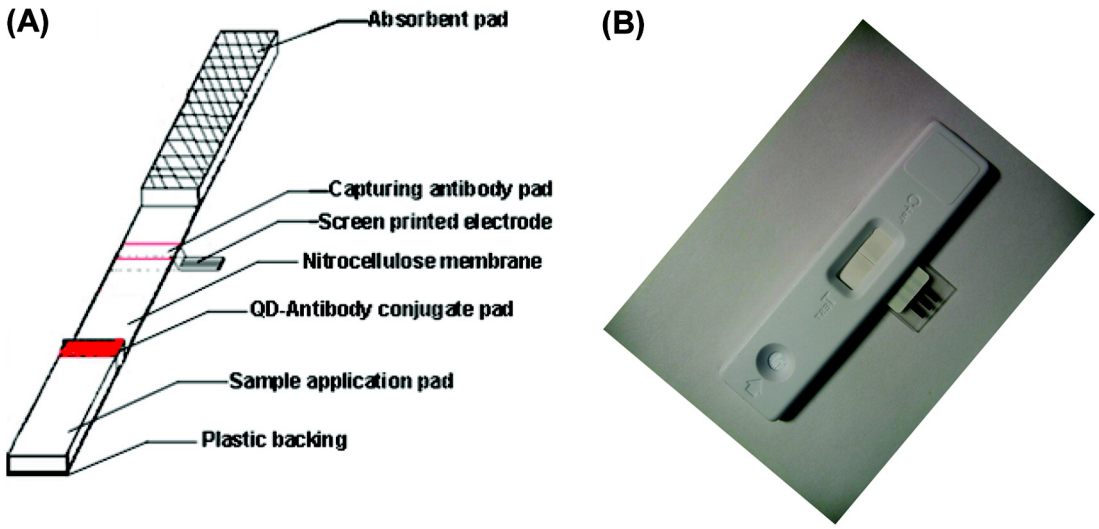

Figure 1.4. Disposable diagnostic device for POCT (**Liu et al., 2007**). Reprinted with permission from ref. **Liu et al., 2007**. Copyright 2007 American Chemical Society.

covering the metals are closely packed. SAM molecules typically have a headgroup that covalently bind to the substrate, an alkyl group chain, and a functional group at the terminal (**Love et al., 2005; Schreiber et al., 2004**). Biological elements can be covalently bound with the functional group of the SAM and become the base of the immunoassay complex construction on the transducer. SAMs are relatively easy to prepare and the thickness is on the order of few nanometers, depending on the alkyl chain length. For the blocking process, bovine serum albumin is commonly used as a passivation of the surface sensing area from non-specific binding (**Angenendt et al., 2002**). Before conducting the analysis, biochemical sample usually need a pretreatment by adjusting its pH with buffer solution. Buffer solution like phosphate buffer saline with pH of 7.4 is typically used to maintain a constant pH and preserve biological activity of the biochemical molecules.

1.2.1 Liquid plug formation for reducing sample volume in microfluidic system

In typical processing of sample in LOC, samples solutions are introduced into the flow channel, manipulated, and then chemical or biological analysis was carried out. For the analysis of one kind of sample solution, a simple structure of one flow channel is necessary. However, if there are many kind of different sample solutions interacted or processed in the device, it becomes very difficult and challenging to manipulate and additional number of flow channels may necessary. On the other hand, delivering all of the sample solutions in continuous flow into the chip even though the sensing region is limited, the consumption of sample

solutions can exceed the intended requirement. To solve such problem, instead of using conventional continuous flow in the chip, forming a liquid plug for each solution is very appealing (**Linder et al., 2005; Han et al., 2009**).

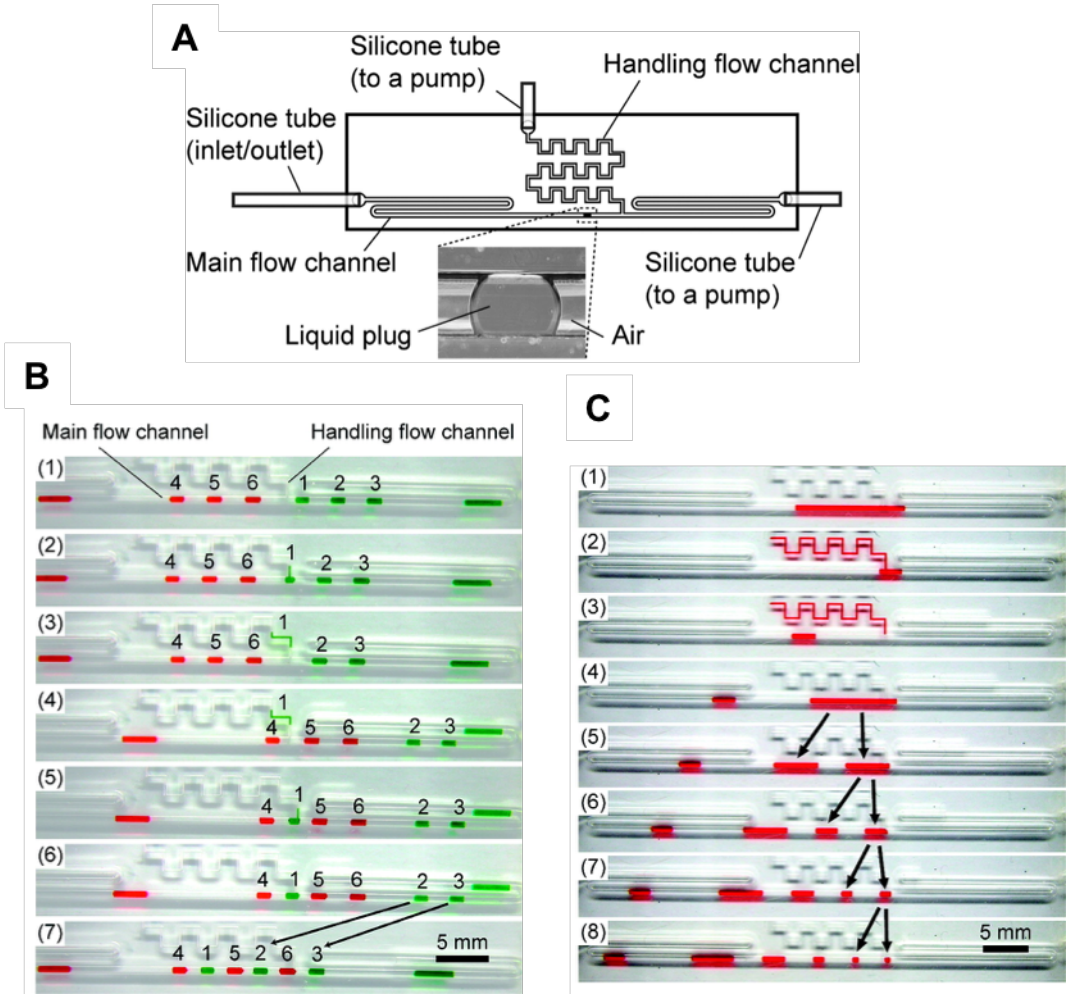

Figure 1.5. Microfluidic device for processing the solution plug (**Sassa et al., 2008**). (A) Construction of the microfluidic device. (B) Manipulation of liquid plugs. (C) Resizing the liquid plug volume. Reprinted with permission from ref. **Sassa et al., 2008**. Copyright 2008 American Chemical Society.

In conventional droplet-based microfluidic system, the droplets were formed by segmenting the sample using immiscible liquid such as oil which cannot mix with the aqueous solutions. In a liquid plug system, the continuous flow is segmented by air instead of using oil. Therefore, it becomes feasible for processing different kinds of sample solutions in the same flow channel or reducing the number of flow channels that is necessary to form in the case of continuous flow. Another benefit is the number of consumed reagents can be minimized using this technique. Through these segmented plugs, the manipulation process such as mixing and splitting of different solution sources can be easily realized. Further division of the plug also possible which lead to the further reduction of the sample volume, thus reducing the samples, reagents and experimental cost. The mixing

principle of different sample solutions is based on circulation movement caused by the friction between the plug and the wall of flow channel. Due to the limited amount of volume, mixing process is complete rapidly than on the basis of laminar flow in the case of conventional continuous flow.

In the previous work (**Sassa et al., 2008**), microfluidic device for processing and manipulation of liquid plug can be easily achieved. **Figure 1.5** shows the construction of the device. Air is used to separate and transport liquid plugs in flow channel. Through the push/pull mechanism by air pump connected to the inlet/outlet of the flow channel and with the help of T-junction flow channel design, the formation, quantitation, segmentation, and transportation of the liquid plugs can be realized. Using such mechanism for plug processing in a microfluidic device, different kinds of sample solution can be processed in the same flow channel.

1.2.2 Development of microfabricated immunosensors for protein detection

Biosensors for immununodiagnostic purposes can be categorized according to their transducers; electrochemical-based, optical-based, and mechanical-based. Optical detection offers a simple labeled detection method for immunosensing purposes. Old product such as lateral flow immunoassays commonly use colorimetric detection method, although the tests are mostly qualitative, and the visibility can be seen only if the presence of analyte exceeds certain concentration (**Xu et al., 2009**). Optical-based detection of the analyte was also conducted using fluorescent experiment. The analyte was bound with the fluorophores material or quantum dots then observe under a fluorescence microscope (**Gervais et al., 2009; Schult et al., 1999; Delehanty et al., 2002**). Surface plasmon resonance (SPR) has commonly used in optical biosensing due to its label-free and real-time capabilities. In SPR technique, the beam of light is reflected on the bottom surface of metal thin film and the reflected light will be measured. The binding of molecules on the metal surface will change the local refractive index and the surface plasmons resonance in the metal. These changes lead to the changes of angle and wavelength of the reflected light (**Li et al., 2010**). Chemiluminescence gain popularity in optical sensor technology. Emitted light intensity as a result of a series of chemical reactions was measured. It typically employs oxidation of luminol reactant to release a reaction product that gives off light (**Yakovleva et al., 2002; Yacoub-George et al., 2002; Wojciechowski et al., 2009**). Absorbance-based method also shows the promising result for low concentration detection of analyte (**Usuba et al., 2016**).

As for mechanical-based transducer, cantilever and quartz crystal microbalance (QCM) are commonly tested for immunosensors. Cantilever can work in two different modes (**McKendry et al., 2002**). In a static mode, the cantilever bends because of the attachment of particle having certain mass or a force acting on it. In a dynamic mode, the frequency of the resonant is monitored and the change due to the attached mass on the structure will be recorded. QCM also highly sensitive to the mass and the material properties of deposited molecular layers (**Tai et al., 2005**). The measuring principle is based on the precise oscillation at their resonant frequency when applying an alternating voltage. Depositions at the surface give a frequency shift and a damping of the oscillation. The frequency shift and the damping/dissipation of the oscillation are captured in real time.

Potentiometric immunosensor as one of electrochemical-based sensing device rely upon the difference of potential that occurs between working electrode and reference electrode that is generated as a results of recognition/interaction event between antibodies and antigens. However, there is a disadvantage using this type as relatively only a small change in potential that can be observed. Sample matrix may also give some interferences which make the observation of this small signal become more difficult (**Purvis et al., 2003**).

Table 1.1. Different immunosensors with their advantages and disadvantages.

Transducer	Method	Analyte	Detection limit	Reference
Electrochemical	Cyclic voltammetry	D-Dimer	20 ng/mL	**Rossier et al., 2001**
		Mouse IgG	10 ng/mL	**Dong et al., 2007**
	Amperometry	Mouse IgG	0.25 fg/mL	**Wang et al., 2001**
		α-fetoprotein	2 ng/mL	**Dai et al., 2007**
		Carcinoembryonic antigen *α*-fetoprotein	0.25 ng/mL 0.13 ng/mL	**Zhang et al., 2009**
		Carcinoembryonic antigen Prostate specific antigen	0.2 ng/mL 2 ng/mL	**Fragoso et al., 2011**
		Insulin	58 pg/mL	**Wang et al., 2003**
		α-fetoprotein Ferritin Carcinoembryonic antigen *β*-human choriogonadotropin	1.4 ng/mL 7.0 ng/mL 1.2 ng/mL 1.8 ng/mL	**Wilson et al., 2006**
		Carcinoembryonic antigen *α*-fetoprotein	30 pg/mL 50 pg/mL	**Qi et al., 2012**
	Potentiometry	Troponin I	10 pg/mL	**Purvis et al., 2003**
	Anodic stripping voltammetry	Carcinoembryonic antigen	1.2 pg/mL	**Ge et al., 2012**
	Electrochemical impedance spectroscopy	Creatine kinase	2.4 pg	**Shin et al., 2016**
Optical	Fluorescence	Chorionic gonadotropin	1 ng/mL	**Schultz et al., 1999**
		Cholera toxin Staphylococcal enterotoxin B Ricin	0.3 ng/mL 2.8 ng/mL 9.1 ng/mL	**Delehanty et al., 2002**
		Interleukin-8 (IL-8)	0.3 ng/mL	**Rendl et al., 2013**
	Chemi-luminescence	Atrazine	0.80 pg/mL	**Yakovleva et al., 2002**
		Staphylococcal enterotoxin B	5 ng/mL	**Yacoub-George et al., 2002**
		Staphylococcal enterotoxin B	0.5 ng/mL	**Wojciechowski et al., 2009**
	Absorbance	Interleukin-2 (IL-2)	50 pg/mL	**Usuba et al., 2016**
	SPR	Ischemia modified albumin	10 pg/mL	**Li et al., 2013**
	Colorimetric	Thrombin	2.5 nM	**Xu et al., 2009**
Mechanical	Cantilever	DNA	Several femtomoles	**McKendry et al., 2002**
	QCM	Dengue virus NS1	1 ng/mL	**Tai et al., 2005**

In amperometric immunosensor, the current change generated by the reduction or oxidation of electroactive species at a fixed potential is observed. These electroactive species are in the form of redox labels which typically the enzymes, as both antigens and antibodies are not electroactive (**Wang et al., 2001; Dai et al., 2007; Zhang et al., 2009; Fragoso et al., 2011; Wang et al., 2003; Qi et al., 2012**). Impedimetric immunosensor detects the change of interfacial conductivity at a fixed potential when specific interaction of antigens by the antibodies immobilized on the transducer surface were occurred (**Shin et al., 2016**). Other electrochemical techniques that were used in the immunosensors are cyclic voltammetry (**Rossier et al., 2001; Dong et al., 2007**) and anodic stripping voltammetry (**Ge et al., 2012**).

Table 1.1 summarized previous works on the development of microfabricated immunosensors for protein detection that have been explained above. Careful selection of the transducer is important when LOC want to be deployed for on-site measurement. Comparing the advantages and disadvantages among three kinds of transducers, electrochemical-based sensors are much reliable and feasible for POC diagnostic in a limited environment (**Chaubey et al., 2002**). Optical- and mechanical-based LOC device typically require strict experimental setup and controlled of surrounding environment, thus limiting the chances for on-site deployment. Majority of the POC diagnostic tools based on electrochemical method used enzymatic labelling and sandwich assay strategies. The advantage of using enzymes as a label is the high selectivity to specific substrate. Other advantage is during the enzymatic reaction, enzymes can release ions, electrons/protons, or light which is measurable.

1.3 Coulometric microfluidic device

The number of publications related to the development of the coulometric microdevice for protein detection is still few if we compare it with devices using other electrochemical methods. From our knowledge, previous works on coulometric devices still not meet a satisfactory level for a high sensitivity detection (**Mizutani et al., 2008; Oh et al., 2016; Bunyakul et al., 2009**). In addition, volume of the reagents consumption was relatively big. Our group has worked intensively on the development of coulometric microdevice for the detection of small molecules.

In our previous work (**Sassa et al., 2010**), a coulometric microdevice for the determination of H_2O_2 in a liquid plug was developed (**Figure 1.6**). Using this device, it was demonstrated that H_2O_2 can be collected more rapidly and efficiently in the restricted space. In amperometry, current decreases rapidly in such a small space, indicating that the analysis becomes increasingly difficult as the volume of the space decreases. This study shows that the background could be reduced by reducing the area of the working electrode. The ratio of the output charge and the background could be increased when using the shallower flow channel, due to more efficient and rapid decomposition of H_2O_2 on the electrode.

A problem in conventional coulometry was that the background charge increases as time lapses. This influences the detection limit, which is obtained with the background value (3σ) will also increase. In this

condition. measurement of the charge in a longer time will not give a lower detection limit. If the analyte is converted into charge rapidly and the charge saturates within a short time, the increase of the background will be minimized. Ikemoto et al. used two flow channels to convert an analyte (H_2O_2) into silver on a platinum

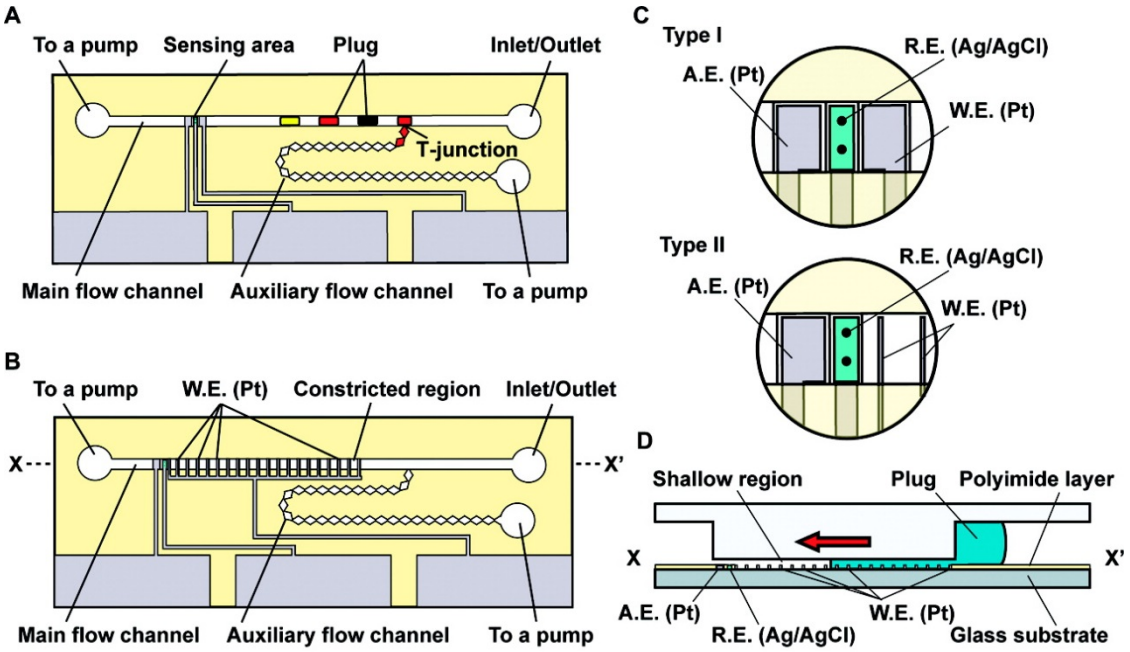

Figure 1.6. Fabricated coulometric microdevices (**Sassa et al., 2010**). (A) Type I device. (B) Type II device. (C) Magnified view of the electrodes construction in Type I device. (D) Magnified view of the electrodes construction in Type II device. Reprinted with permission from ref. **Sassa et al., 2010**. Copyright 2010 American Chemical Society.

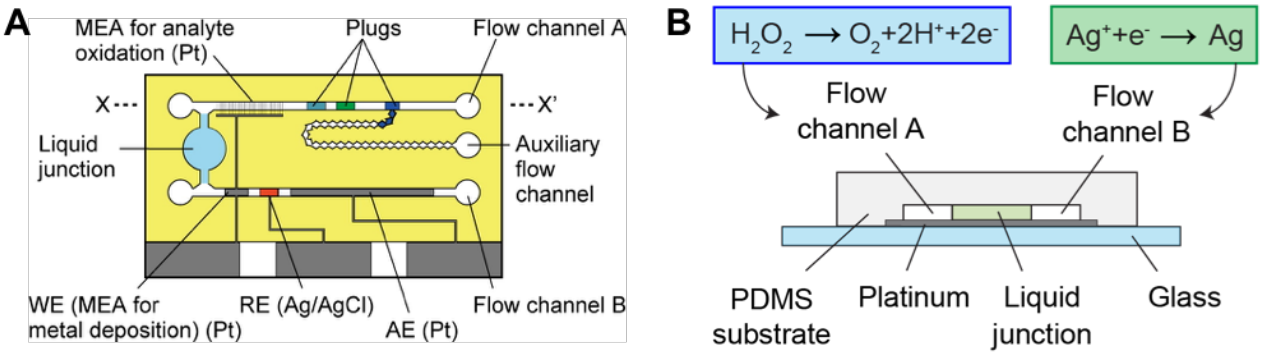

Figure 1.7. Device based on coulometry coupled with silver metallization (**Ikemoto et al., 2016**). (A) Schematic of the fabricated device. (B) Simultaneous oxidation of H_2O_2 and reduction of Ag^+ at mixed potential. Reprinted with permission from ref. **Ikemoto et al., 2016**. Copyright 2016 American Chemical Society.

electrode at a mixed potential (**Figure 1.7B**) and measure the amount of deposited silver by coulometry (**Ikemoto et al., 2016**).

The device used in this study is shown in **Figure 1.7A**. In this device, the information of an analyte (H_2O_2) in one flow channel was converted into the amount of silver deposited in another flow channel. In this device, the structure of the electrodes in the two flow channels was changed to improve collection efficiency of the analyte and minimize the background charge. Interestingly, the response charge was increased rapidly, and the slope was dropped suddenly in the same level of the background within several seconds. It indicates that the deposited silver already removed from the working electrode after the coulometry was conducted (**Figure 1.8**). Such technique can successfully lower the previous detection limit by 1 order of magnitude from the previous study (**Sassa et al., 2010**). l redox reaction.

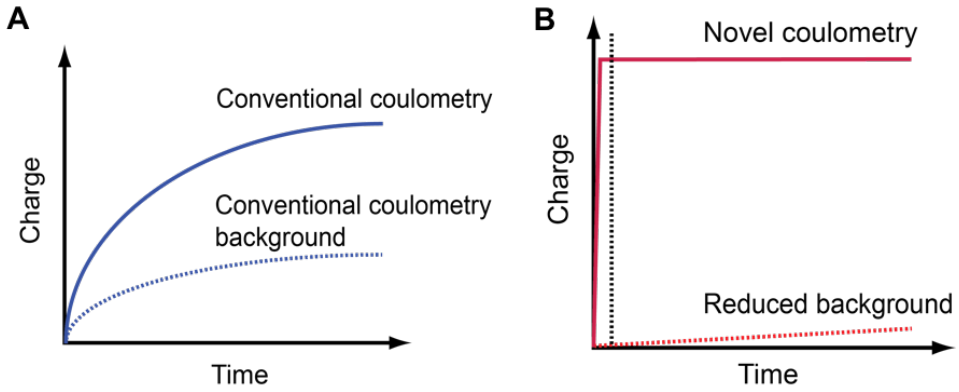

Figure 1.8. Change in the response profiles from (A) conventional coulometry to (B) coulometry coupled with silver metallization.

1.4 Objective of this study

A major objective of this study was to develop coulometric microfluidic devices to realize highly sensitive detection of proteins. In particular, the objective is to provide devices based on coulometry coupled with silver metallization with a high-performance response for immunodiagnostics. The coulometric microdevices were designed to consume only a tiny volume (several µL ranges) of reagents such as antibodies and proteins. Configuration of the works was outlined as follows:

- Development of the protein chip based on coulometry coupled with metallization
- Enhancement of the metallization through the use of metal junction
- Optimization of the immunoassay parameters and structure of the device
- Optimization of the immobilization condition and minimization of adsorption of non-specific protein

Looking at the recent trend, LOC diagnostic tools are at the brink of aiding decentralized testing. These

tools will be brought to patients as their personal monitoring system outside of the hospital and continuous communication with clinicians. In the near future, hopefully our system can enrich the recent methods of developing protein chips for POC diagnostics, especially for the device based on coulometric detection.

Literature cited

Angenendt, P. *Anal. Biochem.* **2002**, *309*, 253-60.

Anna, S. L. et al. *Appl. Phys. Lett.* **2003**, *82*, 364-366.

Attia, U. M. et al. *Microfluid. Nanofluid.* **2009**, *7*, 1-28.

Aumiller, G. D. et al. *J. Appl. Phys.* **1974**, *45*, 4557-4562.

Bartholomeusz, D. et al. *J. Microelectromech. Syst.* **2005**, *14*, 1364-1374.

Becker, H. et al. *Sens. Actuators A* **2000**, *83*, 130-135.

Berry, S. M. et al. *Anal. Chem.* **2012**, *84*, 5518-5523.

Bunyakul N. et al. *Anal. Bioanal. Chem.* **2009**, *393*, 177-186.

Chaubey, A. et al. *Biosens. Bioelectron.* **2002**, *17*, 441-456.

Comina, G. et al. *Lab Chip* **2013**, *14*, 424-430.

Comina, G. et al. *Lab Chip* **2014**, *14*, 2978-2982.

Dai, Z. et al. *Biosens. Bioelectron.* **2007**, *22*, 1700-1706.

Danielsa, J. S. *Electroanalysis* **2008**, *19*, 1239-1257.

Datta, S. et al. *3 Biotech* **2012,** *3*, 1-9.

Delehanty, J. B. et al. *Anal. Chem.* **2002**, *74*, 5681-5687

Dong, H. et al. *Lab Chip* **2007**, *7*, 1752-1758.

Duffy, D. C. D. et al. *Anal. Chem.* **1998**, *70*, 4974-4984.

Dye, C. *Phil. Trans. R. Soc. B* **2014**, *369.1645*, 20130426.

Fragoso, A. et al. Lab Chip **2011**, *11*, 625-631.

Fu, E. et al. *Ann. N. Y. Acad. Sci.* **2007**, *1098*, 335-344.

Ge, S. et al. *Analyst* **2012**, *137*, 4727-4733.

Gervais, L. et al. *Lab Chip* **2009**, *9*, 3330-2009.

Gómez-de Pedro, S. et al. *Sens. Actuators B* **2017**, *245,* 477-483.

Guckenberger, D. J. et al. *Lab Chip* **2015**, *15*, 2364-2378.

Han, Z. et al. *Anal. Chem.* **2009**, *81*, 5840-5845.

Ikemoto, K. et al. *Anal. Chem.,* **2016**, *88*, 9427-9434.

Kunkel, H. G. *Methods Biochem. Anal.* **1954**, *1*, 141-170.

Li, G. et al. *Sensors* **2013**, *13*, 12794-12803.

Linder, V. et al. *Anal. Chem.* **2005**, *77*, 64-71.

Love, J. C. et al. *Chem. Rev.* **2005**, *105*, 1103-1170.

Manz, A. et al. *Sens. Actuators B* **1990**, *1*, 244-248.

Masuda, M. et al. *IEEE Trans. Ind. Appl.* **1989**, *25*, 732-737.

Martin, A. J. et al. *J. Gen. Physiol*. **1951**, *35*, 89-118.

McKendry, R. et al. *Proc. Natl. Acad. Sci.* **2002**, *99*, 9783-9788.

Mizutani, F. et al. *Sens. Actuators B* **2008**, *135*, 304-308.

Murray, C. K. et al. *Clin. Microbiol. Rev.* **2008**, *21*, 97-110.

Nii-Trebi, N. I. *BioMed Res. Int.* **2017**.

Oh, K. W. et al. *J. Micromech. Microeng.* **2006**, *16*, R13-R39.

Oh, J.-M. et al. *Anal. Chem.* **2016**, *88*, 4849-4856.

Pal, R. et al. *Lab Chip* **2005**, *5*, 1024-1032.

Purvis, D. et al. *Biosens. Bioelectron.* **2003**, *18*, 1385-1390.

Qi, H. et al. *Analyst* **2012**, *137*, 393-399.

Rendl, M. et al. *Anal. Chem.* **2013**, *85*, 9469-9477.

Rossier, J. S. et al. *Lab Chip* **2001**, *1*, 153-157.

Samiei, E. et al. *Lab Chip* **2016** *16*, 2376-2396.

Sassa, F. et al. *Anal. Chem.* **2008**, *80*, 6206-6213.

Sassa, F. et al. *Anal. Chem.* **2010**, *82*, 8725-8732.

Schult, K. et al. *Anal. Chem.* **1999**, *71*, 5430-5435.

Schreiber, F. *J. Phys. Condens. Matter* **2004**, *16*, R881-R900.

Shin, S. R. et al. *Anal. Chem.* **2016**, *88*, 10019-10027.

Tai, C.-H. et al. *Biomed. Microdevices* **2007**, *9*, 533-543.

Tai, D.-F. et al. *Anal. Chem.* **2005**, *77*, 5140-5143.

United Nations. *United Nations General Assembly 68th Session* **2013**.

Usuba, R. et al. *ACS Sens.* **2016**, *1*, 979-986.

Walker, G. A. *Lab Chip* **2002**, *2*, 131-134.

Wang, J. et al. *Anal. Chem.* **2001**, *73*, 5323-5327.

Wang, J. et al. *J. Am. Chem. Soc.* **2003**, *125*, 8444-8445.

Whitesides, G. M. *Nature* **2006**, *442*, 368-373.

Wilson, M. S. et al. *Anal. Chem.* **2006**, *78*, 6476-6483.

Woias, P. *Sens. Actuators B* **2005**, *105*, 28-38.

Wojciechowski, J. R. et al. *Anal. Chem.* **2009**, *81*, 3455-3461.

Xu, H. et al. *Anal. Chem.* **2009**, *81*, 669-675.

Yacoub-George, E. et al. *Anal. Chim. Acta* **2002**, *457*, 3-12.

Yager, P. et al. *Natur*e **2006**, *442*, 412-418.

Yakovleva, J. et al. *Anal. Chem.* **2002**, *74*, 2994-3004.

Yalow, R. S. et al. *Nature* **1959**, *115*, 1648-1649.

Zhang, S. et al. *Electrophoresis* **2009**, *30*, 3427-3435.

Chapter 2 Microfluidic device for high-sensitivity coulometric detection of proteins

2.1 Introduction

Electrochemical sensing devices are beneficial for the POCT applications, because they can be fabricated with low cost and easily coupled with microfluidics. Microfluidics is advantageous in the reduction of sample and reagent volumes. Furthermore, processing of the solutions in the form of plugs can further reduce the volume. In analyzing such solution plugs, coulometry is more advantageous than amperometry. Coulometry measures charge that originates from a redox reaction. However, in conventional coulometry, not only the charge that originates from the redox reaction but also the background increases as time elapses, which restricts further improvement of the detection limit. Ideally, the charge that originates from the redox reaction should be increased as much as possible, and the background should be minimized. This can be realized by converting an analyte into deposited metal and measure the amount by coulometry.

2.2 Principle of detection

For a redox pair, dependence of current on the electrode potential can be expressed by the Butler-Volmer equation (**Bard et al., 1980**), which is written as follows

$$j = j_{anodic} + j_{cathodic} = j_0 \cdot \left\{ exp\left[\frac{\alpha_a nF}{RT}\left(E - E_{eq}\right)\right] - exp\left[-\frac{\alpha_c nF}{RT}\left(E - E_{eq}\right)\right]\right\} \qquad (2.1)$$

where

j: current density (A/m^2)

j_o: exchange current density (A/m^2)

E: electrode potential (V)

E_{eq}: equilibrium potential (V)

T: absolute temperature (K)

n: number of electrons involved in the electrode reaction

F: Faraday constant

R: universal gas constant

α_c: cathodic charge transfer coefficient

α_a: anodic charge transfer coefficient.

Figure 2.1 shows the polarization curves derived from the Butler-Volmer equation. The upper part is the curve for the anodic reaction, whereas the lower part of the curve for the cathodic reaction. The point where the anodic and cathodic currents are equal corresponds to the equilibrium state. When two or more redox reactions occur on the same electrode and there is no net current that passes through the electrode-solution interface, the sum of the anodic and cathodic currents must be zero (**Figure 2.2**). The electrode potential under this condition is called the mixed potential. The redox reactions of this kind on a single electrode can be seen in the corrosion of a metal or electroless plating. As mentioned in **Chapter 1**, Ikemoto et al. used metallization technique to improve the performance of a coulometric microfluidic device (**Ikemoto et al., 2016**). In this case, the oxidation of the analyte, H_2O_2, and the deposition of silver occurred on the same platinum electrode in separate flow channels at the mixed potential. The amount of deposited silver was measured by coulometry. By separating the oxidation and reduction reactions into two flow channels, collection efficiency of the analyte was improved, and background was reduced. As a result, sensitivity and detection limit were remarkably improved. In this chapter, the device was used for highly sensitive detection of proteins.

2.3 Experimental Section

2.3.1 Reagents and materials

The following reagents and materials were obtained for fabrication and characterization of the device: positive photoresist (S-1818G) from Dow Chemical (Midland, MI, USA); glass substrate (no. 7740, 3 inch, 500 μm thick) from Corning Japan (Tokyo, Japan); poly(dimethylsiloxane) (PDMS; KE-1300T) and its curing reagent (CAT-1300) from Shin-Etsu Chemical (Tokyo, Japan); thick-film photoresist (SU-8 25) from MicroChem (Westborough, MA, USA); polyclonal goat anti-human alpha-1-fetoprotein antibody (C-19) as a capture antibody, and polyclonal rabbit anti-human alpha-1-fetoprotein antibody (H-140) as a detection antibody, from Santa Cruz Biotechnology (Dallas, TX, USA); human alpha-1-fetoprotein standard from Dako (Tokyo, Japan); glucose oxidase conjugation kit from AbD Serotec (Kidlington, UK); methanol (99.8%), Agarose-L, L-cysteine, 1-ethyl-3-(3-dimethylaminopropyl)-carbodiimide, *N*-hydroxysuccinimide (NHS), bovine serum albumin (BSA), glucose oxidase (GOD) (from *Aspergillus niger*, activity: 200 units/mg), D-glucose, and phosphate buffered saline (PBS; pH 7.4) from Wako Pure Chemical Industries (Osaka, Japan); 5-aminofluorescein (isomer I) from Tokyo Chemical Industry (Tokyo, Japan). Solutions used in the experiments were prepared or diluted with 10 mM PBS.

2.3.2 Device fabrication

Figure 2.3 shows the fabricated device. The device was fabricated on a glass substrate with thin-film electrodes formed by the sputter deposition. A PDMS substrate with a flow channel structure was stacked onto it. There are two flow channels, A and B, in the device where oxidation and reduction occur separately. Rectangular platinum (5.4 mm x 0.6 mm) and gold (4.8 mm x 0.6 mm) electrodes formed in flow channel A were used for oxidizing H_2O_2 and immobilizing capture antibodies, respectively. The height of the flow

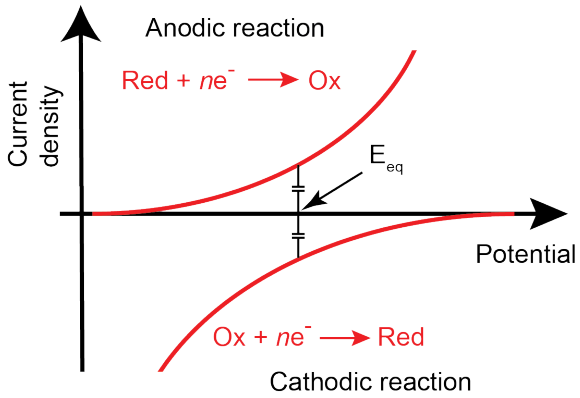

Figure 2.1. Polarization curves of one redox reaction derived from Butler-Volmer equation.

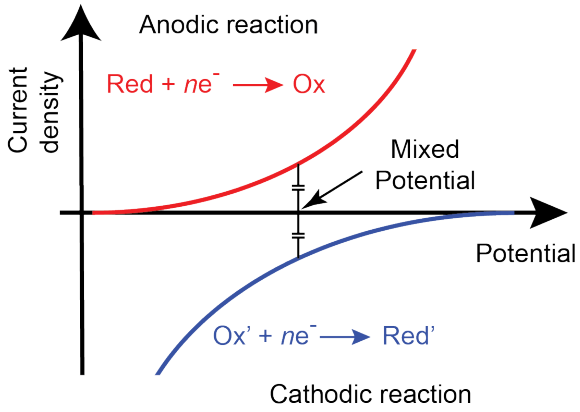

Figure 2.2. Example of a mixed potential between two different redox reactions.

channel over the platinum electrode in flow channel A was reduced to 70 μm to improve collection efficiency. The height of the other portions of the flow channels was 520 μm. The width of these two flow channels were 600 μm. An auxiliary flow channel with rhombuses structure (each rhombus has a volume of 100 nL) was connected to flow channel A to measure the volume of a solution plug. In flow channel B, a platinum working electrode, an Ag/AgCl reference electrode, and a platinum auxiliary electrode were formed for coulometry. The working electrode in flow channel B was connected with the rectangular platinum electrode in flow channel A. A positive photoresist insulating layer with a pinholes structure was formed on the working and reference electrode areas. Twenty-six pinholes (diameter: 30 μm) were formed on the working electrode and three pinholes (diameter: 40 μm) were formed on the reference electrode.

The PDMS substrate with the flow channel structure was fabricated by replica molding using an SU-8 thick-film photoresist mold. The PDMS solution was mixed with the curing solution, and the mixture poured onto the mold substrate. After curing for 30 min at 80 ^{o}C, the PDMS was peeled off from the mold and was cut into chips of an appropriate size. The flow channels were connected with a liquid junction formed by pouring agarose (2%) dissolved in a 1.0 M KCl solution at 80 ^{o}C into the compartment and solidifying it as it cooled down to room temperature. To form the on-chip Ag/AgCl electrode, the silver electrode was immersed in a 0.1 M KCl solution along with a commercial Ag/AgCl reference electrode and a platinum auxiliary electrode. A constant current (50 nA) was applied to the silver electrode for 15 min with magnetic stirring and the growth was monitored via the electrode potential.

2.3.3 Procedure for solution plug processing

Air pressure from microsyringe pumps (IM-9B, Narishige, Japan) was used for moving solutions in the flow channels. The pumps were connected to flow channel A and the auxiliary flow channel through silicone tubes (inner diameter: 500 μm) to form a solution plug in flow channel A **(Sassa et al., 2010)**. **Figure 2.4** shows how plugs are formed. First, a solution to be processed was introduced into the auxiliary flow channel, filling 15 rhombuses (1.5 μL plug volume). The excess solution was flushed out from flow channel A by applying a negative pressure to the inlet. Next, the solution plug whose volume was measured in the auxiliary flow channel was moved onto the gold electrode in flow channel A for incubation. This technique was used for solutions of detection anti-AFP antibodies, AFP, and capture anti-AFP antibodies. For the other solutions, the auxiliary flow channel was not used.

2.3.4 Procedure and optimization for immobilization of capture antibodies

Capture antibodies were immobilized on the gold electrode using a self-assembled monolayer (SAM) of cysteine. For optimization, arrays of gold disk (diameter: 1 mm) formed on a glass substrate were prepared, which were formed by sputter deposition and lift-off process was prepared (**Figure 2.5A**). A PDMS substrate with a simple straight flow channel (width: 1 mm; height: 520 μm) was stacked (**Figure 2.5B**). Next, cysteine (50 mM), carbodiimide (50 mg/mL), and NHS (50 mg/mL) solutions were poured onto the gold disks and

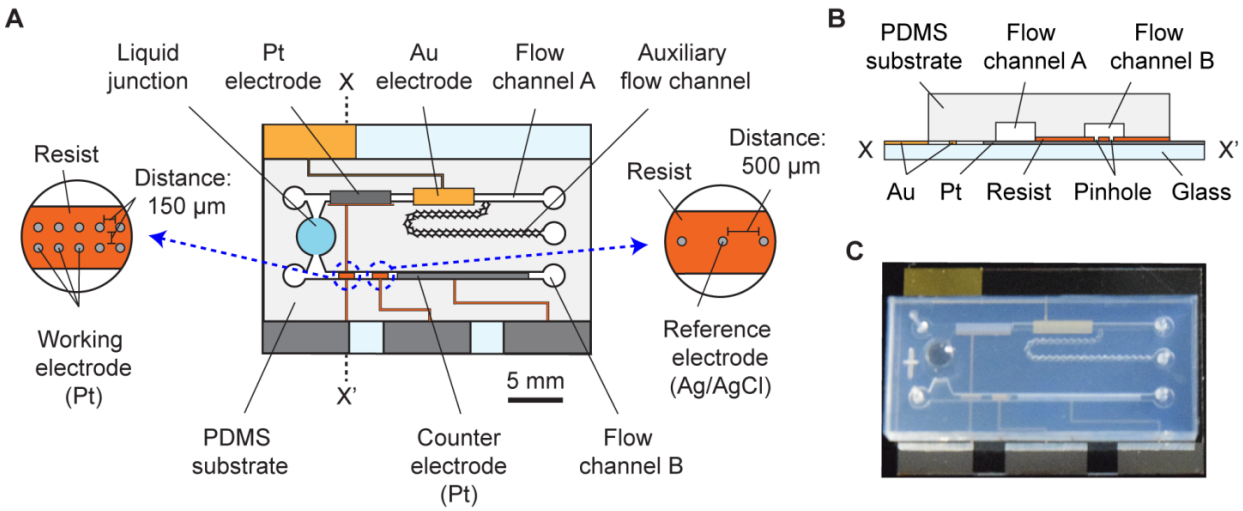

Figure 2.3. Fabricated device for detection of protein based on coulometry coupled with silver metallization. (A) Schematic of the device. (B) Cross section of the device along the line marked X-X' in (A). (C) Photograph of the device. Reprinted with permission from ref. **Anshori et al., 2018**. Copyright 2018 Elsevier.

incubated stepwise to form the SAM layer. The time of incubation (10–90 min) for each of the three reagents were same (**Table 2.1**). The discs were rinsed with PBS after finishing the incubation of each reagent. The ester group formed on the SAM was used to immobilize biomolecules containing amino groups. The optimum condition was found by binding 5-aminofluorescein to the SAM and measuring the fluorescence intensity. 10 μM 5-Aminofluorescein dissolved in absolute methanol was used for this experiment. The incubation time for 5-Aminofluorescein was the same as that of the previous three reagents. The discs were rinsed with distilled water after incubation. For measuring the fluorescence intensity, the PDMS substrate was replaced with a PDMS substrate with square (6 mm × 6 mm) through-holes to be reaction chambers with four gold discs (**Figure 2.5C**). PBS was injected into the chambers, and the chambers were sealed with a cover glass. Olympus IX73 fluorescence microscope (Olympus, Tokyo, Japan) was used for the fluorescence measurements. Before conducting ELISA, capture anti-AFP antibodies were immobilized on the gold electrode. An SAM of cysteine was formed and activated on the gold electrode in flow channel A under the optimum condition. Next, a solution plug of capture anti-AFP antibodies was incubated for 60 min on the gold electrode modified with the SAM. The flow channel was then rinsed with PBS. Finally, a BSA solution (5.0 mg/mL) was introduced into the auxiliary flow channels and flow channel A (except for the Pt electrode) and incubated for 30 min. The flow channels were rinsed with PBS.

2.3.5 Procedure for AFP detection

Figure **2.6** shows the detection principle of the device. Sandwich structures of capture anti-AFP antibodies, AFP, and detection anti-AFP antibodies were formed by incubating the solutions stepwise (**Figure 2.6, step 1**). Each solution was incubated on the gold electrode for 30 min. The flow channel was rinsed with PBS after each incubation step. A glucose plug (3 μL) was then incubated for 30 min on the gold electrode. H_2O_2 was produced by the enzymatic reaction of GOD consuming glucose as a substrate. GOD was used for comparison with the previous device on the H_2O_2 detection.

$$\text{Glucose} + O_2 \xrightarrow{\text{GOD}} \text{Gluconolactone} + H_2O_2$$

Next, the plug was moved onto the platinum electrode in flow channel A. In flow channel B, a 1.0 M $AgNO_3$ solution containing 0.1 M KNO_3 was introduced. The oxidation of H_2O_2 (**Figure 2.6, Step 2-1**) and the reduction of Ag^+ ions (deposition of silver) (**Figure 2.6, Step 2-2**) proceeded simultaneously. The deposition of silver was conducted for 5 min. Both solutions were flushed and the flow channels were washed with distilled water. Finally, in flow channel B, a 0.1 M KCl solution was introduced, and coulometry was conducted. +0.7 V was applied to the working electrode (vs. Ag/AgCl on the chip) using a potentiostat (Autolab PGATAT12, Metrohm Autolab, Netherlands). **Table 2.2** summarized the experimental steps and the incubation time of each step. Background charge was calculated by two methods. In the first method, a 0.1 M

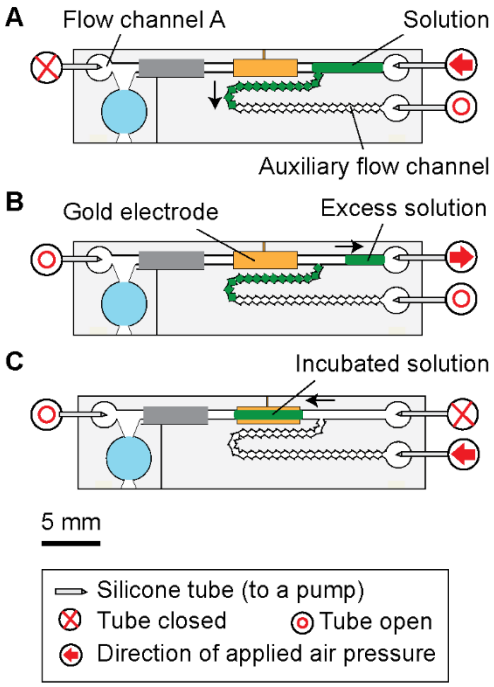

Figure 2.4. Procedure for forming the solution plug and incubate it onto gold electrode with silver metallization. Reprinted with permission from ref. **Anshori et al., 2018**. Copyright 2018 Elsevier.

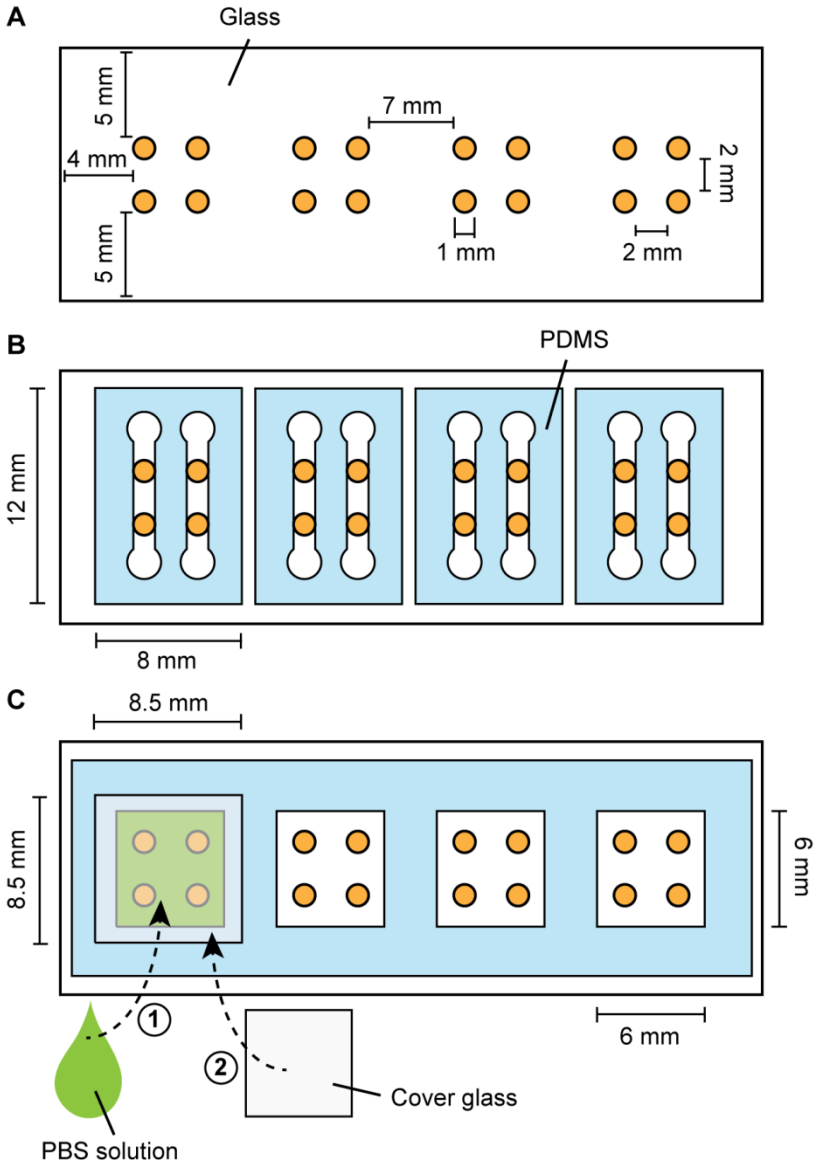

Figure 2.5. Setup of the device for optimization of capture antibodies on the gold electrode. Reprinted with permission from ref. **Anshori et al., 2018**. Copyright 2018 Elsevier.

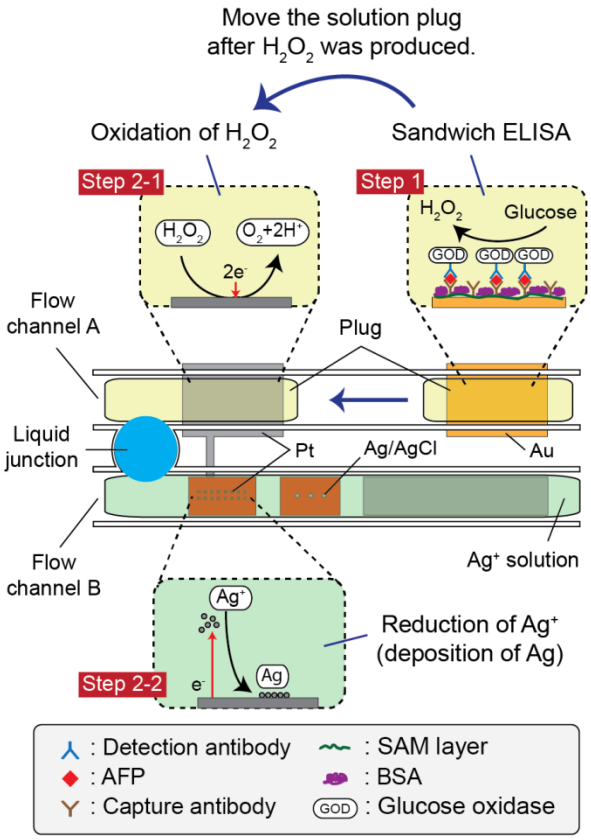

Figure 2.6. Detection principle using the device. After the glucose plug incubated on the gold electrode has produced H_2O_2, the plug moved to the platinum electrode (step 1). Oxidation of H_2O_2 (step 2-1) and deposition of silver (step 2-2) then occurred. Reprinted with permission from ref. **Anshori et al., 2018**. Copyright 2018 Elsevier.

KCl solution was introduced into flow channel A and a 1.0 M $AgNO_3$ solution was introduced into flow channel B. Next, coulometry was conducted to measure the amount of deposited silver on the pinhole working electrode in flow channel B. In the second method, detection anti-AFP antibodies labeled with GOD were introduced into the gold electrode region with the immobilized capture antibodies without incubating AFP analyte. The flow channel was washed with PBS and then glucose solution was introduced onto the gold electrode region. After 30 min incubation, the plug was moved to the sensing region and coulometry was conducted.

2.4 Result and Discussion

2.4.1 Performance of the device as a coulometric detector

Figure 2.7A shows typical response profiles obtained with H_2O_2 standard solutions. Charge increased rapidly and saturated thereafter. The rapid charge increase indicates that silver was oxidized rapidly. The small electrode area on the working electrode in flow channel B minimized the background. After the initial rapid increase, the subsequent gradual increase was close to the background charge, suggesting that all the deposited silver was oxidized (dissolved) and was no longer present on the working electrode; at this stage, only the background charge was recorded. **Figure 2.7B** shows the dependence of charge on the concentration of H_2O_2. The values at 7 s were plotted in this Figure. A linear relationship was confirmed between the charge and the concentration ($R^2 = 0.989$). The lower detection limit (3σ) was 119 nM. The background was higher than in our previous study. This may be attributed to the larger electrode area in flow channel A. However, the origin of reactions other than the oxidation of H_2O_2 have not currently been identified.

2.4.2 Optimization of the immobilization of antibodies

Incubation times of three solutions used in the formation of the SAM were optimized. **Figure 2.8** shows the ratio of the intensity of fluorescence from 5-aminofluorescein bound to the SAM on the gold disk with respect to its background obtained using the bare gold disk. After 60 min, the intensity was saturated. Based on the result, incubations with solutions of cysteine, carbodiimide, and NHS were conducted for 60 min. To obtain the optimum concentration of glucose, GOD was immobilized on the SAM. Glucose plug was incubated on the gold electrode surface and the enzymatic reaction product (H_2O_2) was detected by coulometry. The charge increased with the increase in glucose concentration, and saturated at concentrations higher than 50mM (**Figure 2.9**). The result is reasonable considering that the Michaelis constant of GOD from *Aspergillus Niger* is 33 mM (**Swoboda, et al., 1965**). From the result, we decided to use a 200 mM glucose solution.

2.4.3 Detection of AFP

AFP was determined by sandwich ELISA. In this device, the site for immunoreaction and the site for detection were separated to avoid the decrease in the activity of the platinum electrode because of the SAM

formation. **Figure 2.10** shows the response to AFP of different concentrations. Similar to the case of H_2O_2 detection, the charge increased rapidly then the slope decreased rapidly to the same level of the background. This indicates that the product of the enzymatic reaction could be detected. **Figure 2.11** shows dependence of charge on AFP concentration. Based on this, the calculated detection limit was 1.4 ng/mL (3σ). However, the background charge was different between the first and second methods. With the first method where 0.1 M KCl was used in flow channel A, the average background charge was 63 nC. On the other hand, with the second method where the ELISA was conducted by omitting AFP, the average background charge was 280 nC. It was considered that nonspecific binding of detection anti-AFP antibodies occurred on the walls of the flow channel. Further optimization is necessary to overcome this problem.

2.4.4 Sensitivity improvement for obtaining lower limit of detection (LOD)

Detection limit was improved by increasing the length of time for the enzymatic reaction in the final step of ELISA. Here, the use of the solution plug is very advantageous. In a stationary plug, the enzymatic reaction product accumulates in the limited volume of the plug. If the size of the plug is much larger or if the solution is continuously flowed, the enzymatic reaction product is diluted. On the other hand, a problem with small plugs is the evaporation of water. The glucose plug shrank by 5.1% (n=5) after 30 min incubation, which indicates that approximately 0.15 μL of plug volume was lost during this incubation period. To solve this problem, the plug was replaced with another fresh plug every 30 min. **Figure 2.12** shows the charge changes by increasing the time for the enzymatic reaction by the replacement. The estimated detection limit of AFP for 120 min enzymatic reaction was 0.4 ng/mL. The inset shows the ratio of glucose consumed in a single plug during the enzymatic reaction for 30 min. The consumption of glucose in the plug was negligible (consumption ratio: 7.4×10^{-5}). Therefore, if the evaporation of water does not pose serious problems, the reaction time could be increased more using a single plug.

Table **2.3** shows the comparison of the performance of our device with that of previous coulometric devices for protein detection. Our device gives a better detection limit than other microfabricated devices. However, a direct comparison is not easy because there were many factors to be considered. Nevertheless, the performance of the device is satisfactory at the present stage, considering the solution volumes and further improvements that could be included.

2.5 Conclusions

A highly sensitive analytical microdevice based on coulometry coupled with silver metallization for the detection of proteins was developed. In this system, the oxidation of an enzymatic reaction product from an ELISA process and the reduction of silver ions occurred simultaneously on platinum electrodes in different flow channels connected with a liquid junction. The sensitivity can be increased by increasing the enzymatic

reaction time. The detection limit of 0.4 ng/mL was achieved for AFP. Further improvements could be achieved by reducing the background and limiting the loss of detection antibodies and analyte proteins.

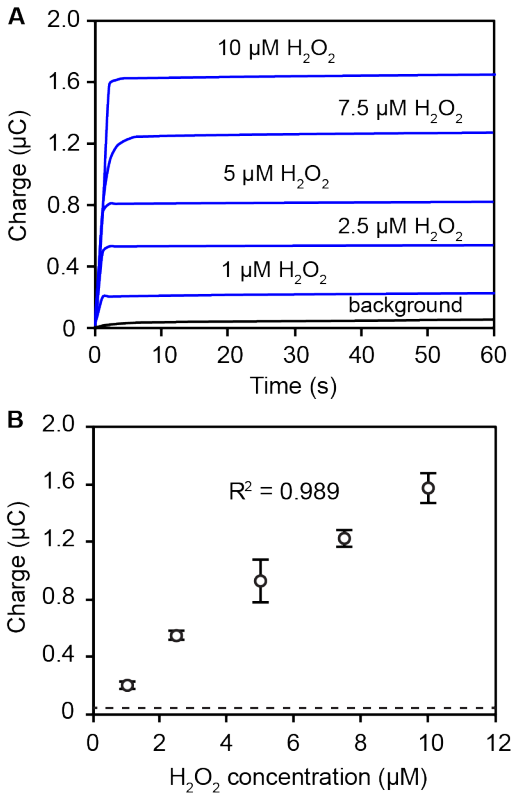

Figure 2.7. Detection of H_2O_2 using the device. (A) Charge response curves of H_2O_2 solutions of different concentrations. (B) Dependence of generated charge (time = 7 s) on H_2O_2 concentration. Data are shown as means ± standard deviations (n = 5). Dashed line indicates the background charge.

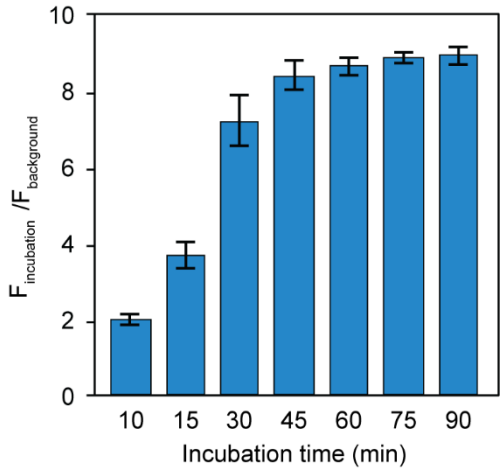

Figure 2.8. Fluorescence intensity of 5-aminofluorescein bound to the gold discs. Reprinted with permission from ref. **Anshori et al., 2018**. Copyright 2018 Elsevier.

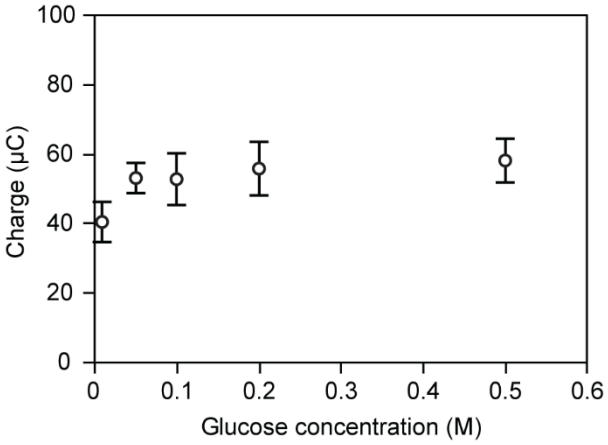

Figure 2.9. Dependence of the coulometric charge on glucose concentration. Reprinted with permission from ref. **Anshori et al., 2018**. Copyright 2018 Elsevier.

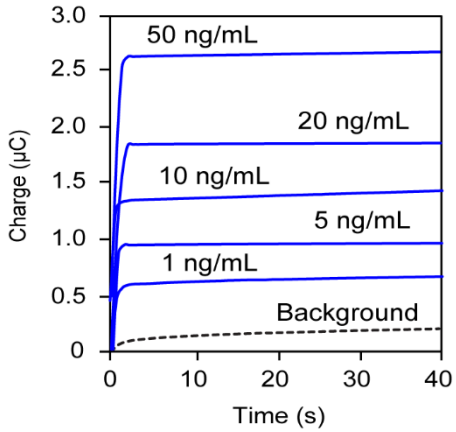

Figure 2.10. Response profiles of coulometric charge on different AFP concentrations. Reprinted with permission from ref. **Anshori et al., 2018**. Copyright 2018 Elsevier.

rations

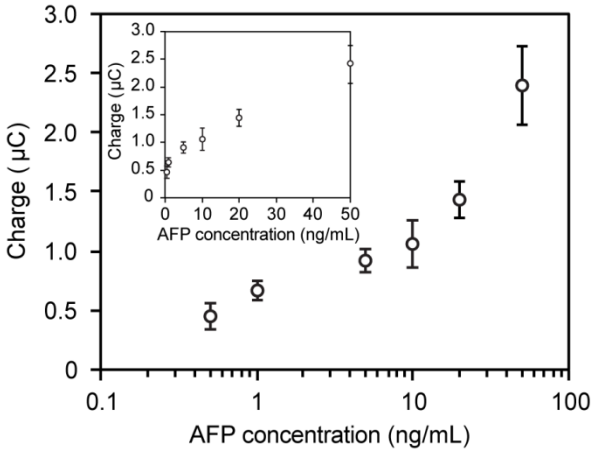

Figure 2.11. Charge dependence on the AFP concentration plotted on a logarithmic scale and the data plotted on a linear scale (inset). Error bar shows the standard deviation (n=5). Reprinted with permission from ref. **Anshori et al., 2018**. Copyright 2018 Elsevier.

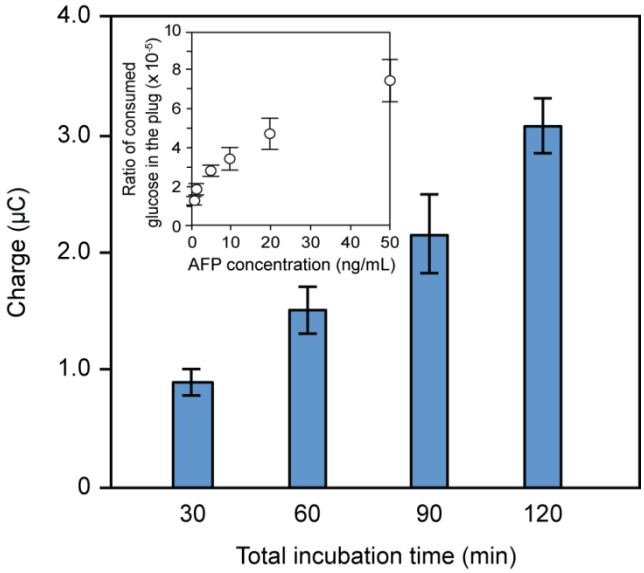

Figure 2.12. Coulometric charges obtained from the ELISA process. Inset shows the consumption of glucose during the enzymatic reaction. Reprinted with permission from ref. **Anshori et al., 2018**. Copyright 2018 Elsevier.

Table 2.1. Incubation times for forming the SAM and the binding of fluorophore to the linker

Step	Incubation time (min)						
1. Cysteine	10	15	30	45	60	75	90
2. Carbodiimide	10	15	30	45	60	75	90
3. NHS	10	15	30	45	60	75	90
4. 5-aminofluorescein	10	15	30	45	60	75	90

Table 2.2. Step of each procedure and its incubation time

Step	Incubation time (min)
1. AFP	30
2. Detection anti-AFP antibody labeled with GOD	30
3. Glucose	30
4. H_2O_2 oxidation/Ag deposition	5

Table 2.3. Previous works on coulometric devices for protein detection

Analyte	Detection limit	Remarks	Reference
Insulin	0.01 ng/mL	- Not microfabricated. Working electrode: disk of 3 mm diameter - Reagents used for sensing: 1 mL	(**Mizutani et al., 2008**)
Horseradish peroxidase-avidin	Not mentioned	- Linear range: 0.1–0.5 µg/mL - Sample volume: 40 µL	(**Oh et al., 2016**)
Cholera toxin subunit B	1.0 ng/mL	- Non-stationary sample solution. Flow rate: 0.1 µL/min. - Sample volume: 4 µL	(**Bunyakul et al., 2009**)
AFP	0.4 ng/mL	- Plug-based system - Sample volume: 1.5 µL	This work

Literature Cited

Bard, A. J. et al. *Electrochemical methods: fundamentals and applications Vol. 2*, Wiley, **1980**.

Bunyakul, N. et al. *Anal. Bioanal. Chem.* **2009**, *393*, 177-186.

Bygbjerg, I. C. *Science* **2012**, *337*, 1499-1501.

Dai, Z. et al. *Biosens. Bioelectron.* **2007**, *22*, 1700-1706.

Ikemoto, K. et al. *Anal. Chem.* **2016**, *88*, 9427-9434.

Ko, J. S. et al. *Lab Chip* **2003**, *3*, 106-113.

Lim, T. K. et al. *Anal. Chem.* **2003**, *75*, 3316-3321.

Mizutani, F. et al. *Sens. Actuators B* **2008**, *135*, 304-308.

Oh, J.-M. et al. *Anal. Chem.* **2016**, *88*, 4849-4856.

Rendl, M. et al. *Anal. Chem.* **2013**, *85*, 9469-9477.

Sassa, F. et al. *Anal. Chem.* **2008**, *80*, 6206-6213.

Swoboda, B. E. P. et al. *Biol. Chem.* **1965**, *240*, 2209-2215.

Usuba, R. et al. *ACS Sens.* **2016**, *1*, 979-986.

Yakovleva, J. et al. *Anal. Chem.* **2002**, *74*, 2994-3004.

Zhang, S. et al. *Electrophoresis* **2009**, *30*, 3427-3435.

Chapter 3 Enhancement of detection sensitivity by metal junction

3.1 Introduction

Our previous work of coulometry coupled with silver metallization was based on simultaneous oxidation of H_2O_2 and reduction of Ag^+ at a mixed potential (**Ikemoto, et al., 2016**). In this device, two flow channels were connected with a liquid junction. Polarization curves of these two redox reactions are shown in **Figure 3.1A**. In this case, we cannot expect the enhancement of current by any means. However, if the electrode potentials for the oxidation and reduction reactions can be manipulated separately as shown in **Figure 3.1B**, the current will increase. In the study explained in this chapter, we investigated the possibility of using a metal wire as an alternative to a liquid junction. Several methods were tested to obtain sufficient electrode potential difference between one electrode where the oxidation reaction occurred and another electrode where the reduction reaction occurred. Manipulation of the electrode potentials was focused in the direction of higher oxidation potential and lower reduction potential to obtain higher anodic and cathodic currents (**Figure 3.1B**). The challenge, advantage, and disadvantage of each method were discussed.

3.2 Theory

Figure 3.2 shows the similar device with our previous work (**Ikemoto, et al., 2016**) with a metal wire connecting the two flow channels. When the liquid junction is replaced with the metal junction, four reactions need to be taken into consideration; oxidation of H_2O_2, reduction of Ag/AgCl, oxidation of Ag/AgCl, and reduction of Ag^+. Here, let the electrode potential of the working electrode in flow channel A, metal wire potential in flow channel A, metal wire potential in flow channel B, and working electrode potential in flow channel B as $\Delta\psi_1$, $\Delta\psi_4$, $\Delta\psi_3$, and $\Delta\psi_2$ with respect to the solutions at their locations (**Figure 3.3**). The relation between these potentials can be described as follows

$$\Delta\psi_1 - \Delta\psi_2 + \Delta\psi_3 - \Delta\psi_4 = 0 \quad (1)$$

or

$$\Delta\psi_1 - \Delta\psi_2 = \Delta\psi_4 - \Delta\psi_3 = \Delta E \quad (2)$$

With this relation, the potentials of the electrodes $\Delta\psi_1$ and $\Delta\psi_2$ in flow channel A and in flow channel B can be controlled. From the polarization curves derived using Butler-Volmer equation, mixed potential occurs when the anodic current and the cathodic current from different redox reactions are equal. These four electrode potentials allow three conditions in the system to flexibly controlled the amount of deposited silver, either decreasing or increasing from the case of using liquid junction (**Figure 3.4**). In case 1, the potential of the platinum electrode in flow channel A ($\Delta\psi_1$) is the same as that of the potential of the platinum electrode in

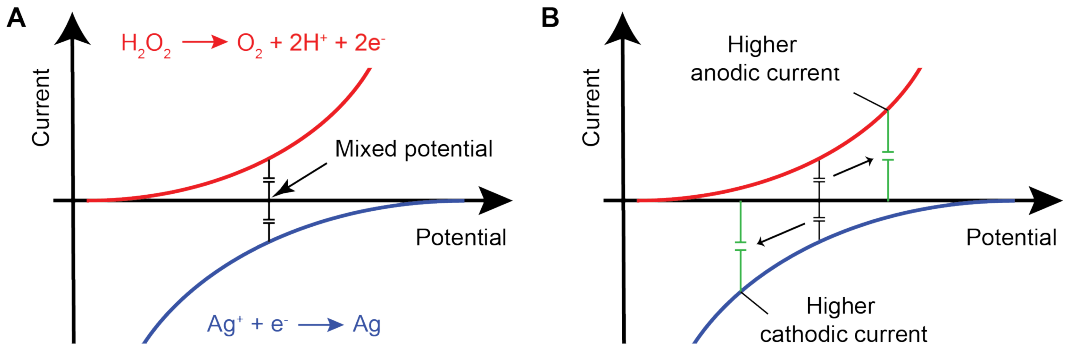

Figure 3.1. Polarization curves of mixed potential in (A) normal condition and (B) enhanced condition.

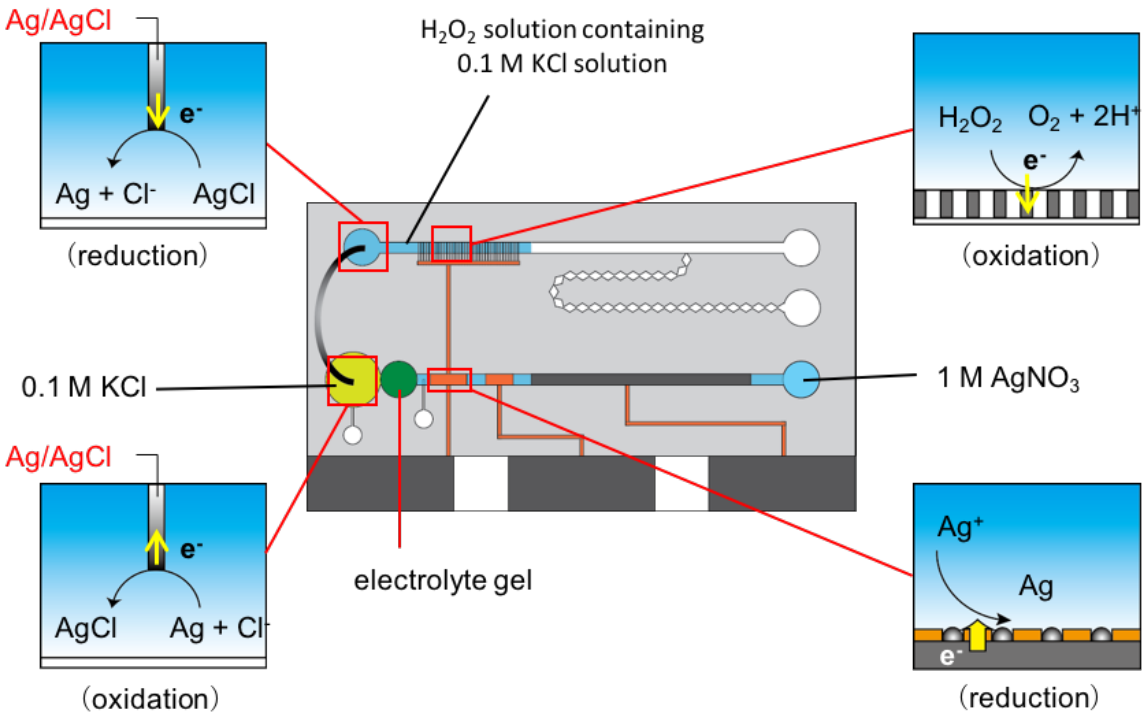

Figure 3.2. Reactions which occurred on each electrode positions when using metal junction for connecting two flow channels. There are four reactions occurred in the device; oxidation of H_2O_2, reduction of AgCl, oxidation of silver, and reduction of Ag^+.

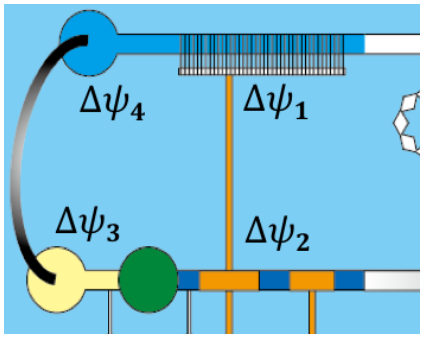

Figure 3.3. Location of four electrode potentials on the device connected with metal junction.

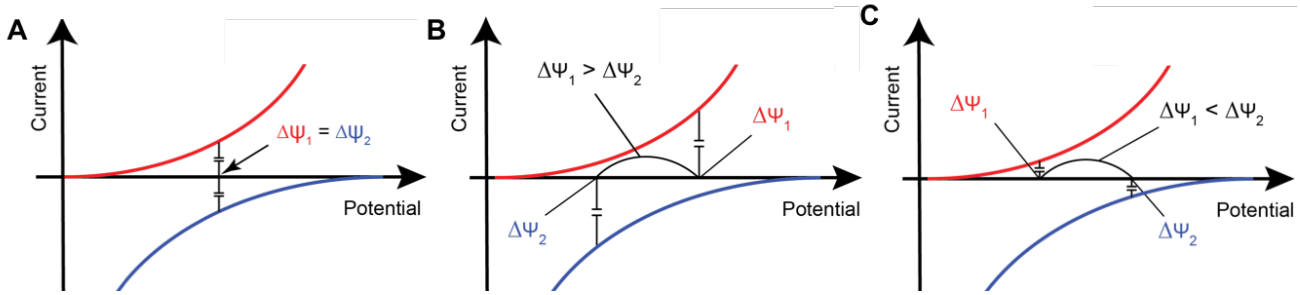

Figure 3.4. Three conditions that could be obtained when using the metal junction connecting two flow channels. (A) Condition where $\Delta\psi_1 = \Delta\psi_2$, same with the case of using liquid junction connecting two flow channels. (B) Condition where $\Delta\psi_1 > \Delta\psi_2$, the generated currents were increased. (C) Condition where $\Delta\psi_1 < \Delta\psi_2$, the generated currents were decreased.

flow channel B ($\Delta\psi_2$) (**Figure 3.4A)**. Case 1 is similar to the case of the previous device (**Ikemoto et al., 2016**) that uses the liquid junction. In case 2, when $\Delta\psi_3 < \Delta\psi_4$ or $\Delta E > 0$, $\Delta\psi_1 > \Delta\psi_2$. In this case, the generated current is expected to increase, as shown on **Figure 3.4B**. Finally, in case 3, when $\Delta\psi_3 > \Delta\psi_4$ or $\Delta E < 0$, $\Delta\psi_1 < \Delta\psi_2$. In this case, the current will decrease (**Figure 3.4C**). To obtain a highly sensitive detection of the analyte in a system based on the coulometry coupled with silver metallization, the amount of the deposited silver need to be increased. For such condition, the generated current need to be higher and follow the case 2 ($\Delta\psi_1 > \Delta\psi_2$). Therefore, the difference between electrode potentials also needs to be sufficiently high. In this chapter, the parameters that can increase the generated current (or case 2) were studied in detail.

3.3 Experimental Section

3.3.1 Reagents and materials

The following materials and reagents were used for device fabrication and characterization: glass substrate (no. 7740, 3 inch, 500 µm thick) from Corning Japan (Tokyo, Japan); poly(dimethylsiloxane) (PDMS; KE-1300T) and its curing reagent (CAT-1300) from Shin-Etsu Chemical (Tokyo, Japan); positive photoresist (S-1818G) from Dow Chemical (Midland, MI, USA); thick-film photoresist (SU-8 25) from MicroChem (Westborough, MA, USA) ; potassium chloride (KCl), hydrogen peroxide (H_2O_2), zinc chloride ($ZnCl_2$), ammonium chloride (NH_4Cl_2), nickel (II) sulfate hexahydrate ($NiSO_4.6H_2O$), nickel (II) chloride hexahydrate ($NiCl.6H_2O$), trisodium citrate dehydrate ($C_6H_5Na_3O_7.2H_2O$), silver nitrate ($AgNO_3$), potassium nitrate (KNO_3), and phosphate buffered saline (PBS; pH 7.4) from Wako Pure Chemical Industries (Osaka, Japan); PVA-SbQ, (SPP-H13) from Toyo Gosei (Chiba, Japan); silver wire (diameter: 1.0 mm) from Nilaco Corporation (Tokyo, Japan).

3.3.2 Fabrication of the device

Thin-film electrodes were formed on a glass substrate by sputter deposition. The structure of the fluidic channel was created with PDMS by replica molding using mold patterns of the thick-film photoresist (SU-8 25). The PDMS substrate was stacked on the glass substrate. The device has two flow channels, A and B, where the oxidation and reduction reactions occur separately. The flow channels were 70 µm high and 600 µm wide. An array of platinum electrodes, 10 µm wide and 130 µm interelectrode distances from edge to edge, was formed in flow channel A. In flow channel B, the platinum working electrode of had 26 pinholes, 10 µm diameter, formed using the positive photoresist as an insulating layer (**Figure 3.5**). A Ag/AgCl reference electrode (3 pinholes) and a platinum auxiliary electrode were also formed in flow channel B. Formation of the reference electrode was same as that explained in section 2.2.2. For the formation of the liquid junction, PVA-SbQ was mixed with a 0.2 M KCl solution (1:1 weight ratio). The mixture was injected. into the liquid junction compartment (diameter: 2 mm) and was exposed to ultraviolet light for 1 min to be cured. An open chamber (diameter: 3 mm) to insert one-end of the silver wire was formed on the left portion of flow channel

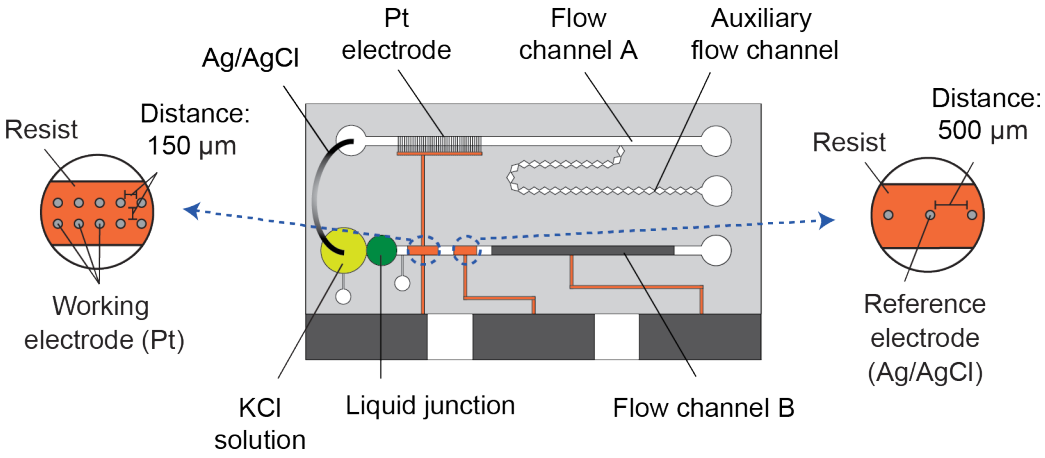

Figure 3.5. Schematic of the coulometric device with a metal junction connecting the two flow channels.

A. Compartment of KCl solution in flow channel B also has a diameter of 3 mm to place another one-end of the silver wire (**Figure 3.5**).

3.3.3 Deposition of AgCl on the silver wire

To grow AgCl on the silver wire, a 1-cm long silver wire was immersed in a 0.1 M KCl solution in a beaker and platinum plate was used as an auxiliary electrode. A constant current (200 μA) was applied for 10 min with respect to the commercial reference Ag/AgCl electrode.

3.3.4 Deposition of zinc or nickel at one end of the silver wire

To form zinc at one end of the silver wire, 0.5 cm wire was immersed in a zinc planting solution which consists of 1.8 M $ZnCl_2$ and 4.9 M NH_4Cl. Then a constant current (−0.005 A) was applied for 2 min with respect to platinum electrode. To form nickel at one end of the silver wire, about 0.5 cm of wire was immersed in a nickel plating solution which consist of $NiSO_4.6H_2O$ 280g/L, $NiCl.6H_2O$ 45g/L, and $C_6H_5Na_3O_7.2H_2O$ 30 g/L. Then a constant current (−0.005 A) was applied for 2 min with respect to a platinum electrode.

3.3.5 Measurement of the working electrode potential

To check the change of electrode potentials ($\Delta\psi_1$ and $\Delta\psi_2$) measured with respect to solution, we measure the electrode potentials with respect to a commercial reference electrode. The latter potentials will be referred to as $\Delta\varphi_1$ and $\Delta\varphi_2$ to differentiate them $\Delta\psi_1$ and $\Delta\psi_2$. In the first case, working electrode potential in flow channel A with respect to a commercial reference electrode was measured (**Figure 3.6A**). A 10 μM H_2O_2 solution (10 μL) was injected into flow channel A. A 0.1 M KCl solution was injected into the electrolyte compartment in flow channel B (left side of the liquid junction). A 1.0 M $AgNO_3$ solution was injected into flow channel B (right side of the liquid junction). The two flow channels then connected by the Ag/AgCl wire. A commercial Ag/AgCl reference electrode (2080A-06T, Horiba, Kyoto, Japan) was inserted into the right inlet of the flow channel A and connected to the reference electrode of potentiostat (AutoLab PGSTAT12, Eco Chemie, Utrecht, Netherlands). Platinum working electrode was connected to the working electrode of potentiostat. Potential measurement of working electrode was then started. In the second case, the potential of the working electrode in flow channel B was measured using a similar experimental setup. In this case, the commercial reference electrode was inserted into the right inlet of the flow channel B.

3.3.6 Procedure for coulometry

After the formation of electrolyte gel of PVA-SbQ in the liquid junction compartment of flow channel B, a H_2O_2 solution (volume: 10 μL; concentration: 10 μM) containing KCl was introduced into flow channel A and 0.1 M KCl solution were injected in the electrolyte compartment of flow channel B (left side of the liquid

junction). Next, two sides of the silver wire were inserted in flow channels A and B. Then, a 1.0 M $AgNO_3$ solution was injected into flow channel B and silver was deposited. The solutions were flushed and the flow channels were washed with pure water. Finally, a 0.1 M KCl solution was injected into flow channel B and coulometry was conducted by applying +0.7 V to the working electrode with respect to the on-chip Ag/AgCl reference electrode. The procedure for coulometry for metal junction modified with nickel or zinc is similar. In this case, however, one end of the silver wire was modified with nickel or zinc. **Figure 3.7** shows the setup of the experiment and the location of the silver wire.

3.3.7 Procedure for coulometry by applying the external voltage source

Figure **3.8A** shows the simplified schematic of this experiment. **Figure 3.8B** shows the setup. After the formation of electrolyte gel in the liquid junction compartment of flow channel B, H_2O_2 containing KCl was introduced into flow channel A and 0.1 M KCl solution were injected into the electrolyte compartment of flow channel B. Next, a Ag/AgCl wire was inserted into the flow channel A (left inlet) and was connected to the working electrode terminal of the potentiostat. Another Ag/AgCl wire was inserted into the 0.1 M KCl compartment of flow channel B and was connected to the reference electrode terminal of the potentiostat. A 1.0 M $AgNO_3$ solution was then injected into flow channel B, and silver deposition was started by applying a potential for a predetermined time. The solutions were flushed and the flow channels were washed with pure water. Finally, a 0.1 M KCl solution was injected in flow channel B and coulometry was conducted by applying +0.7 V with respect to on-chip Ag/AgCl reference electrode of the device.

3.4 Results and discussion

3.4.1 Shifting mixed potential by changing the electrolyte concentration of analyte

In this experiment, we investigated the effect of changing the electrolyte concentration contained in the analyte. Here, the concentration of KCl solution containing H_2O_2 (volume: 10 µL; concentration: 10 µM) was changed (**Takie, 2018**). First, the electrode potentials in flow channel A ($\Delta\varphi_1$) and flow channel B ($\Delta\varphi_2$) were measured. **Figure 3.9** shows that the electrode potential $\Delta\varphi_1$ was more positive than $\Delta\varphi_2$ with KCl of a lower concentration (0.01 M). The coulometric charge was expected to increase in this case. When using 0.1 M KCl, $\Delta\varphi_1 = \Delta\varphi_2$, which is same as the case of using liquid junction connecting the flow channel A and flow channel B. Finally, when KCl concentration is 1 M, $\Delta\varphi_1 < \Delta\varphi_2$. Next, coulometry was conducted. **Figure 3.10** shows results obtained with KCl solutions of different concentrations in flow channel A. Our prediction was confirmed. Using a low concentration of electrolyte (KCl) in the analyte in flow channel A could shift the mixed potential and increase the current, thus increasing the amount of deposited silver on the working electrode in flow channel B.

However, from **Figure 3.9** it can be seen that the difference between $\Delta\varphi_1$ and $\Delta\varphi_2$ was small (<100 mV). To obtain more deposited silver under such condition is not possible. Due to this reason, further increasing the

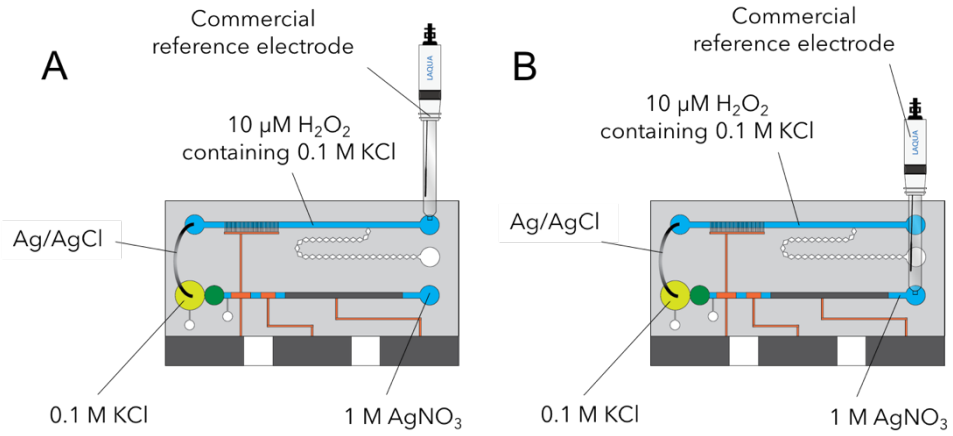

Figure 3.6. Procedure of measuring the working potential (A) in flow channel A and (B) in flow channel B.

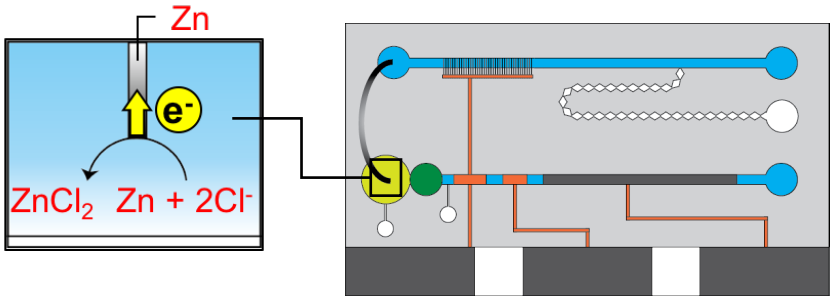

Figure 3.7. Experimental setup for coulometry using the metal wire modified with different metal (nickel or zinc). Expanded view shows the reaction that occurs in the electrolyte compartment during silver deposition.

amount of deposited silver by using much lower concentration of the electrolyte in the analyte was not preferable.

3.4.2 Shifting mixed potential by modifying the metal junction

From this experiment, the mixed potential can be shifted to increase the amount of deposited silver by modifying one end of the metal wire with another metal to obtain a higher electrode potential difference than that in the previous method. Nickel or zinc was deposited on one end of the metal wire. Standard electrode potentials of nickel ($E^0 = -0.257$ V) and zinc ($E^0 = -0.7626$ V) are more negative than silver ($E^0 = 0.7991$ V). When both sides of the wire are Ag/AgCl electrodes, the range of the potential difference that can be adjusted is limited. However, by replacing the AgCl layer with zinc or nickel, the potential difference will be larger and the oxidation and reduction reactions can be enhanced. To check the effect of using these metals, the potential of the platinum electrodes of flow channel A ($\Delta\varphi_1$) and of flow channel B ($\Delta\varphi_2$) were measured. **Figure 3.11** shows the result. The difference of electrode potentials between $\Delta\varphi_1$ and $\Delta\varphi_2$ was −0.06 V. By replacing AgCl on one end of the silver wire with nickel or zinc, the difference of electrode potentials between $\Delta\varphi_1$ and $\Delta\varphi_2$ became +0.16 V in case of nickel or +0.62 V in case of zinc. From this result, $\Delta\varphi_1 - \Delta\varphi_2 > 0$ which suggest the increased of the generated current.

Next, we conducted coulometry to detect H_2O_2. A 10 μM H_2O_2 solution (10 μL) containing 0.1 M KCl was used. **Figure 3.12** shows the results. Modifying one end of the silver wire with zinc gave a much higher response than with AgCl and nickel. The coulometric response signals of zinc-modified wire are typically unsaturated within a short time as in the case of typical signals in coulometry coupled with silver metallization. It is considered that a portion of deposited silver was remained on the pinholes working electrode in flow channel B. Although the difference between $\Delta\varphi_1$ and $\Delta\varphi_2$ was much increased in the case of using zinc and giving a high output charge, controlling the value of $\Delta\varphi_1$ and $\Delta\varphi_2$ by careful selection of the appropriate metal to be deposited is still impractical and not preferable.

3.4.3 Shifting mixed potential by applying the external voltage source

In this experiment, the potential of the platinum electrodes in flow channel A and B were shifted by applying a potential difference between flow channel A with respect to the flow channel B (**Figure 3.8A**). In this case, when a negative voltage is applied to the Ag/AgCl wire placed in the flow channel A (acts as a working electrode) with respect to the Ag/AgCl wire placed in KCl compartment (acts as a reference electrode), the electrons will move from the electrode of flow channel A to the electrode of flow channel B. As a result, silver is deposited on the working electrode in flow channel B.

The voltage was changed from −0.1 V to −0.8 V, and silver was deposited for 5 min the working electrode in flow channel B. A10 μM H_2O_2 solution (10 μL) was used. **Figure 3.13** shows that at a potential higher than −0.6 V the coulometric response was not saturated. It means that some portions of deposited silver on the

working electrode were still remained even after the coulometry (applying +0.7 V) for 60 s. The inspection under the microscope confirmed this condition. Next, the potential of −0.1 V to −0.6 V was tested for 5 min deposition of silver. **Figure 3.14** shows the dependence of charge on different applied potentials. Applying −0.6 V gave the highest charge among others. We also tested the deposition time of silver on the working electrode in flow channel B at 3, 5, and 10 min while applying −0.4, −0.5, and −0.6 V. By increasing the incubation time, the amount of deposited silver was also increased; shown by the increase of output charge (**Figure 3.15**). Using the applied potentials of −0.4, −0.5, and −0.6 V, detection of the H_2O_2 solution was conducted by collecting the deposited silver for 10 min and H_2O_2 concentrations of 1, 2, 5, and 10 μM were tested (**Figure 3.16**). It is clearly seen that using −0.6 V of applied potential could give the highest output charge than by using −0.5 V and −0.4 V. Further detection of H_2O_2 at a lower concentration from 100 nM to 1 μM was tested. **Figure 3.17** shows a good linear relationship between the concentration of H_2O_2 and output charge. Limit of detection of 2.4 nM (3σ) was achieved using this strategy. This strategy shows much simpler control of the silver deposition in a coulometry coupled with silver metallization. The limit of detection for H_2O_2 measurement was improved ten times than our previous work (**Ikemoto, et al., 2016**).

3.5 Conclusions

In this work, we introduced methods for controlling the amount of deposited silver in coulometry coupled with metallization. Methods for obtaining a high generating current were investigated in this chapter. In the first method, the concentration of the electrolyte in flow channel A was changed while keeping the same concentration of KCl in the electrolyte compartment. However, large potential difference on both ends of the silver wire could not be obtained using this method. Next method is changing one end of the metal junction located in the electrolyte compartment to obtain a larger electrode potentials difference. Although the difference has increased, this strategy still impractical and relatively difficult to control the amount of deposited silver. The last method was found to be simpler. The metal wire that connecting flow channel A and B was replaced with two wires connected to the external voltage source. The amount of deposited silver could be controlled easier by selecting the preferable applied voltage. Such system successfully shows the flexibility to control the redox reaction occurred in another part of the electrode.

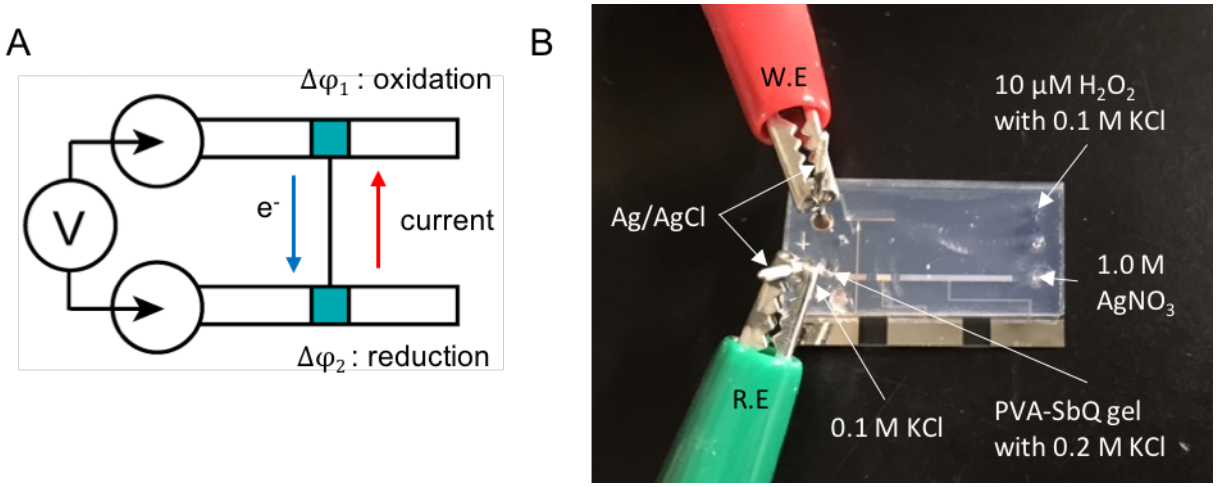

Figure 3.8. Accumulation of the deposited silver through applying external voltage. (A) Mechanism of the silver deposition accumulation. (B) Experimental setup for applying external voltage.

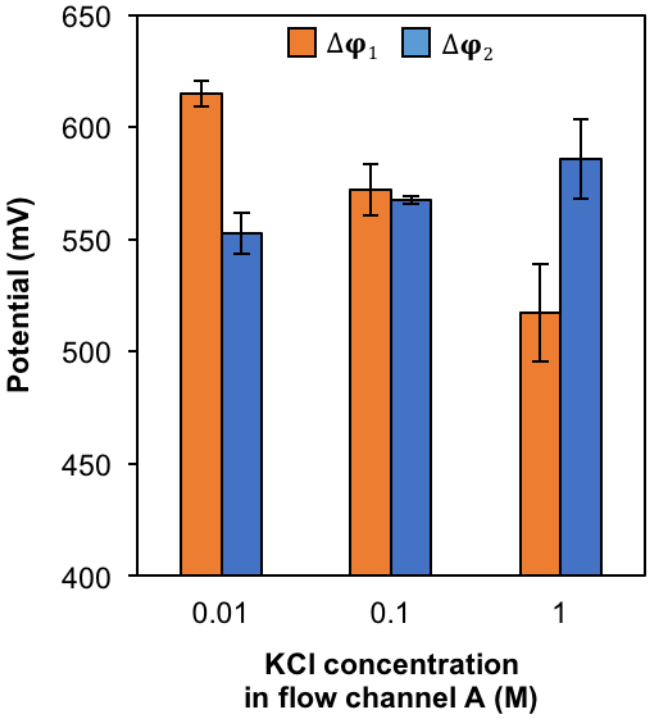

Figure 3.9. Electrode potentials $\Delta\varphi_1$ and $\Delta\varphi_2$ on different KCl concentration in flow channel A.

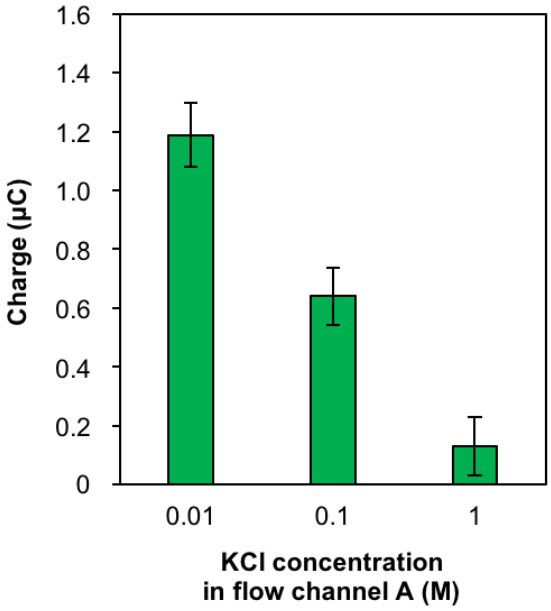

Figure 3.10. Output charge of the device when using different concentrations of KCl in flow channel A.

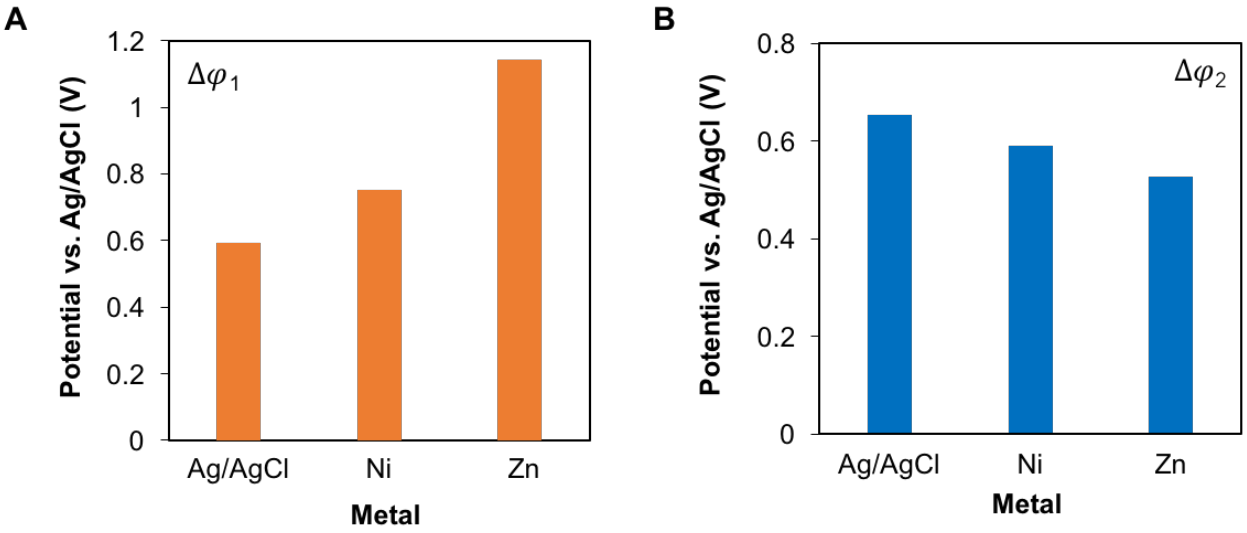

Figure 3.11. Electrode potentials change of working electrode (A) in flow channel A and (B) in flow channel B with respect to the commercial reference electrode when one end of the wire was deposited with metals other than AgCl.

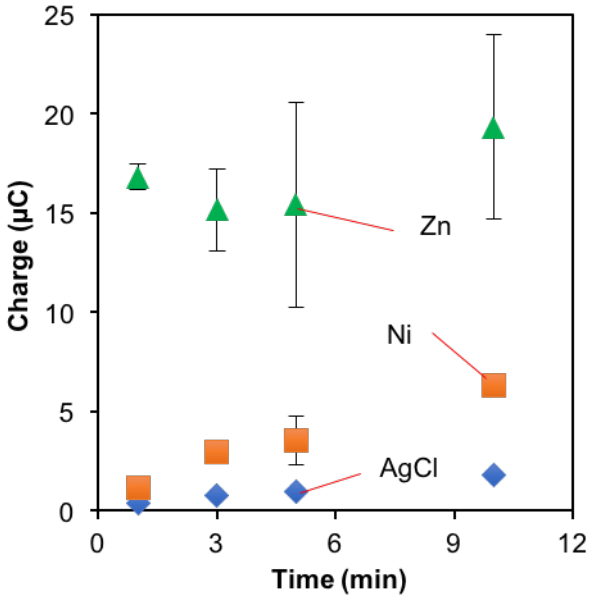

Figure 3.12. Dependence of silver deposition time with coulometric charges on different metal junctions. Modifying the silver wire with nickel or zinc increased the amount of deposited silver.

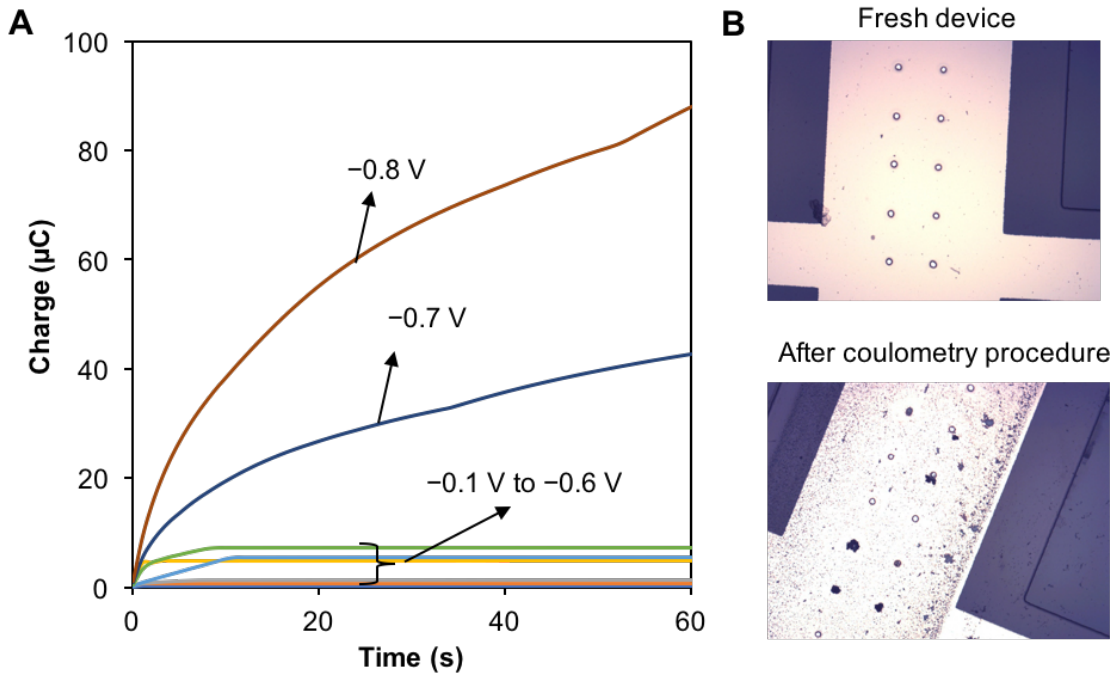

Figure 3.13. Applying a range of an external potential on the setup in Figure 3.5. (A) Coulometric response profiles from −0.1 V to −0.8 V for 5 min deposition of silver. (B) Condition of the pinholes on fresh device and after coulometry procedure for silver deposition using applied potential of −0.7 V.

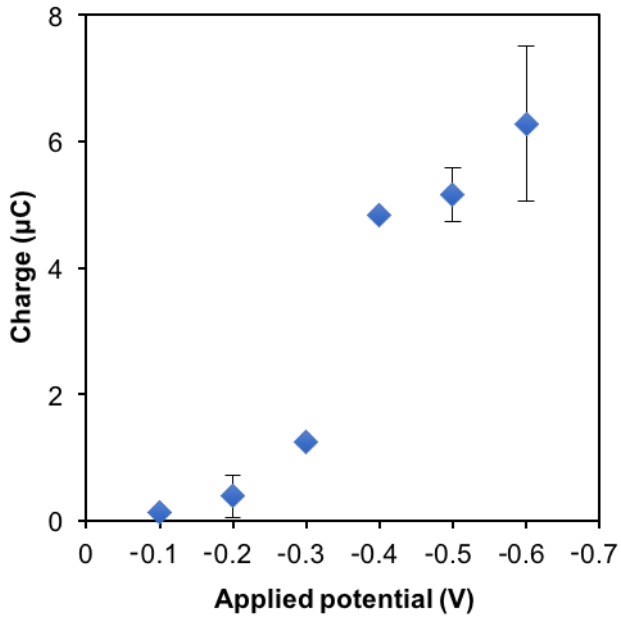

Figure 3.14. Coulometric charge after 5 min silver deposition by applying external potential from −0.1 V to −0.6 V.

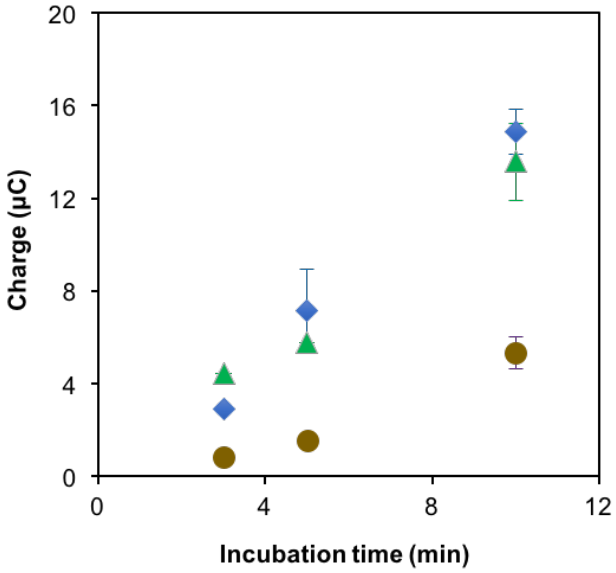

Figure 3.15. Dependence of the incubation time with coulometric charge of −0.4 V (brown color), −0.5 V (green color), and −0.6 V (blue color).

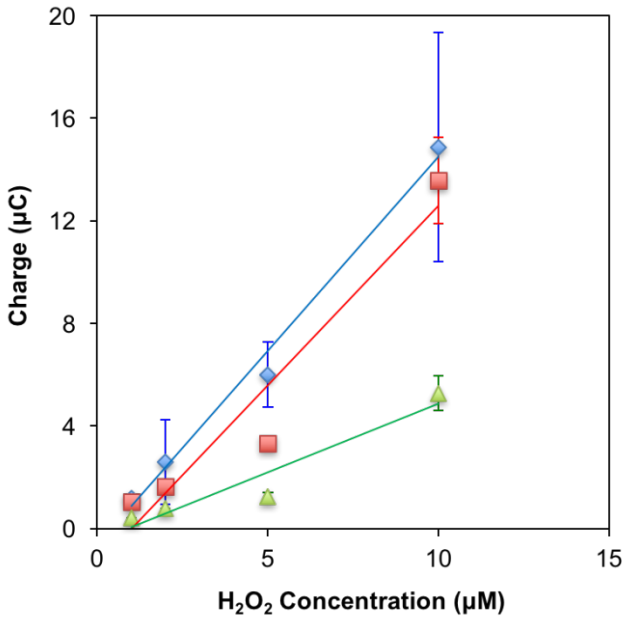

Figure 3.16. Dependence of the output charges with different H_2O_2 concentrations on −0.4 V (green color), −0.5V (orange color), and −0.6 V (blue color) of applied potentials.

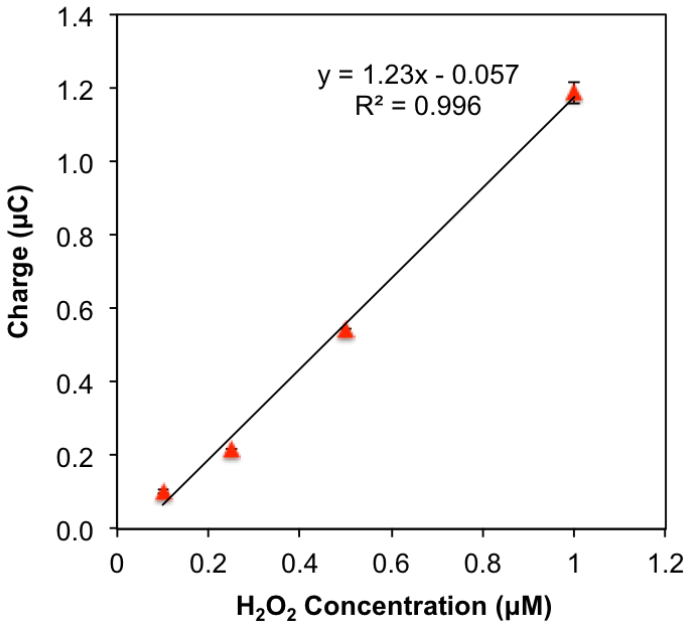

Figure 3.17. Dependence of the output charge with different H_2O_2 concentrations on −0.6 V of applied potentials.

Literature cited

Ikemoto, K. et al. *Anal. Chem.,* **2016**, *88*, 9427−9434.

Takie, S. *Master Thesis,* Graduate School of Pure and Applied Sciences, University of Tsukuba, **2018**.

Chapter 4 Improvement strategies of the coulometric microdevice for protein detection

4.1 Introduction

In our previous work in **Chapter 2**, there were several problems which need to be addressed. A problem is evident in **Figure 2.7**. The background charge for the detection of AFP was much larger than that for the detection of H_2O_2. A major cause of this is probably the non-specific binding of proteins to the PDMS walls during the incubation process of ELISA. To reduce the background, device structure and fabrication were optimized. First, blocking process with BSA was optimized and structure of the working electrode was modified. Second, modification of the flow channel for measurement of the plug. There was a possibility of the losses of protein during the measurement of the plug in the rhombus structure in an auxiliary flow channel.

Along with this, from the study of **Chapter 3**, techniques to enhance the signal were demonstrated. The reduction of silver ion could be increased by replacing a liquid junction with a metal junction and shift the electrode potentials from the mixed potential. In this chapter, we tried the detection of AFP by applying a voltage between the two flow channels to enhance the sensitivity using a device with optimized structures. Finally, redox cycling was also used to improve detection sensitivity.

4.2 Experimental section

4.2.1 Reagents and materials

The following materials and reagents were used for device fabrication and characterization: glass substrate (no. 7740, 3 inch, 500 μm thick) from Corning Japan (Tokyo, Japan); poly(dimethylsiloxane) (PDMS; KE-1300T) and its curing reagent (CAT-1300) from Shin-Etsu Chemical (Tokyo, Japan); positive photoresist (S-1818G) from Dow Chemical (Midland, MI, USA); thick-film photoresist (SU-8 25) from MicroChem (Westborough, MA, USA); potassium chloride (KCl), hydrogen peroxide (H_2O_2), zinc chloride ($ZnCl_2$), ammonium chloride (NH_4Cl_2), nickel (II) sulfate hexahydrate ($NiSO_4.6H_2O$), nickel (II) chloride hexahydrate ($NiCl.6H_2O$), trisodium citrate dehydrate ($C_6H_5Na_3O_7.2H_2O$), silver nitrate ($AgNO_3$), potassium nitrate (KNO_3), *p*-aminophenol (PAP), and phosphate buffered saline (PBS; pH 7.4) from Wako Pure Chemical Industries (Osaka, Japan); PVA-SbQ, (SPP-H13) from Toyo Gosei (Chiba, Japan); silver wire (diameter: 1.0 mm) from Nilaco Corporation (Tokyo, Japan); polyclonal goat anti-human alpha-1-fetoprotein antibody (C-19), as a capture antibody, and polyclonal rabbit anti-human alpha-1-fetoprotein antibody (H-140), as a detection antibody, from Santa Cruz Biotechnology (Dallas, TX, USA); human alpha-1-fetoprotein standard from Dako (Tokyo, Japan); alkaline phosphatase (ALP) conjugation kit from Dojindo Chemical (Tokyo, Japan); methanol (99.8%), Agarose-L, L-cysteine, 1-ethyl-3-(3-dimethylaminopropyl)-carbodiimide, *N*-hydroxysuccinimide (NHS), bovine serum albumin (BSA), glucose oxidase (GOD) (from *Aspergillus niger*, activity: 200 units/mg), D-glucose, and phosphate buffered saline (PBS; pH 7.4) from Wako Pure Chemical

Industries (Osaka, Japan); 4-aminophenylphosphate monosodium salt hydrate (PAPP) from Enzo Life Sciences (Farmingdale, NY, USA); 5-aminofluorescein (isomer I) from Tokyo Chemical Industry (Tokyo, Japan).

4.2.2 Fabrication of the device

Fabrication process of the device was basically the same as that explained in **Section 2.3.2** or **Section 3.3.2**. For the optimization of the device described in **Chapter 2**, the same procedure explained in **Section 2.3.4** was followed. For the experiment using device with the metal junction, fabrication was the same as that explained in **Section 3.3.2**. Details of the device will be explained in related sections.

4.2.3 Optimization of the blocking process for ELISA

Blocking process using BSA was optimized by fluorescence measurement. An Olympus IX73 fluorescence microscope (Olympus, Tokyo, Japan) was used for this experiment. A thin PDMS substrate with a through-hole at the center was stacked on a flat PDMS substrate (**Figure 4.1**). A droplet of solution was injected into the through-hole. Finally, the compartment was covered with a cover glass and fluorescence measurement was conducted. For the background measurement, a droplet of PBS solution was directly placed on the compartment and fluorescence measurement was conducted. To estimate non-specifically adsorbed proteins on the wall of PDMS flow channels, 5-Aminofluorescein solution was incubated for 30 min. The solution then flushed out and the compartment was rinsed. PBS was then injected onto the compartment, and the fluorescence measurement was conducted. To optimize the incubation time for BSA, a BSA solution (5.0 mg/mL) was incubated in the compartment for a certain length of time. After rinsing the compartment, a 5-aminofluorescein solution of 10 μM was incubated for 30 min, followed by rinsing the compartment. Finally, PBS was injected into the compartment and the fluorescence measurement was conducted.

4.2.4 Optimization of the plug volume

In the detection of proteins using the device in **Chapter 2**, the plug of the glucose solution (3 μL) was larger than the minimum volume of the plug to cover the entire area of the gold electrode (1.5 μL). The enzymatic reaction product in the plug can be accumulated more effectively by reducing the plug volume. In this study, the volume of the glucose plug was reduced to 1.5 μL (**Figure 4.2**). Its effect on the background and response charge was examined.

4.2.5 Optimization of the device structure for the plug volume measurement

Structure of the device used in **Chapter 2** for processing of the solution plug was modified to minimize

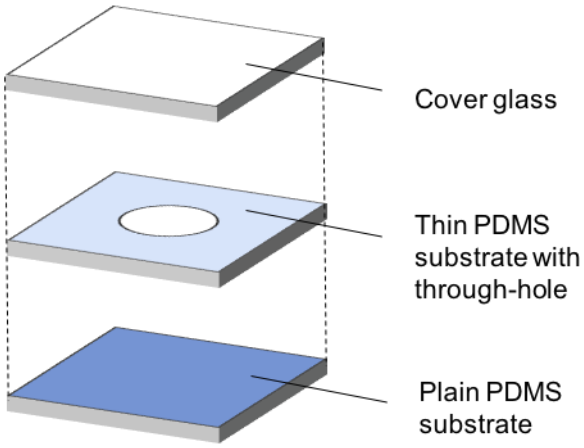

Figure 4.1. Device used for optimizing blocking with BSA in ELISA.

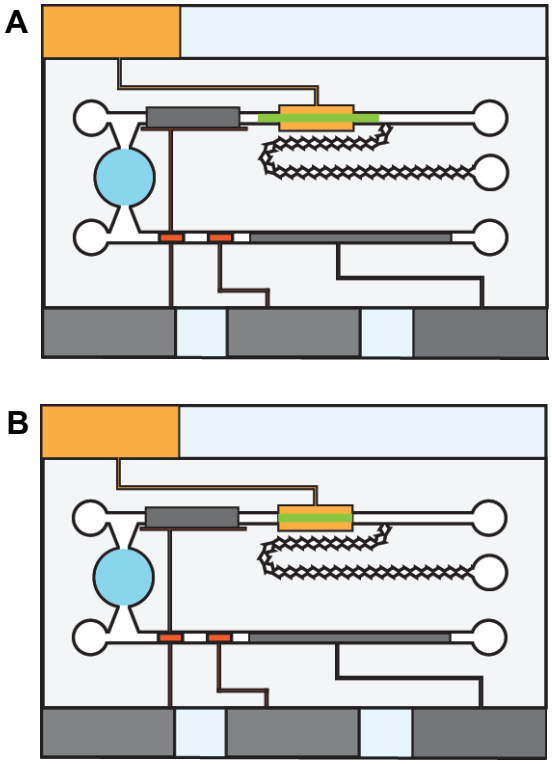

Figure 4.2. Plug size optimization. Plug volume of glucose substrate was reduced from 3 µL (A) to 1.5 µL (B).

the loss of analyte proteins during the measurement of the plug volume. In the modified structure, the auxiliary flow channel with the rhombus structure was removed. **Figure 4.3** shows the modified structure of flow channel A to measure the volume of the plug. The plug volume was measured between two air vents. **Figure 4.4** shows the procedure for processing the plug. First, the solution was introduced into flow channel A from the right inlet. A hydrophobic negative resist pattern help stop the solution when it reached the left air vent. The right air vent was used to cut the solution by applying air pressure. The separated plug was flushed out of flow channel A. A 1.5 µL of a solution plug was measured between these two air vents.

4.2.6 Optimization of the structure of the working electrode in flow channel A

Working electrode structure in flow channel A was modified from the rectangle to comb-like shape (2nd modification). The width of each electrode strip was 30 µm. Total number of electrode strips was 40 and the electrode span the same distance (edge-to-edge) as the previous rectangular electrode (**Figure 4.5**). The flow channel structure explained in **Section 4.2.5** was also used in this design.

4.2.7 Optimization of working electrode in flow channel B

Pinholes working electrode in flow channel B were optimized in two ways; the number of pinholes and the diameter of pinholes. In the first case, the numbers of pinholes of 26, 12, 6, and 2 were tested. In the second case, the diameters of pinholes of 20, 10, 8, 5, and 3 µm were tested. The device from the previous work (**Ikemoto et al., 2016**) was modified for this experiment. For the measurement of the H_2O_2, the procedure follows **Section 2.3.5**.

4.2.8 Detection of AFP using the optimized parameters

Detection of AFP was conducted using the device with optimized structures and methods mentioned from **Section 4.2.3** to **Section 4.2.7**. Also, the technique introduced in **Section 3.3.7** to enhance silver deposition through applying external potential between the two flow channels was used. **Figure 4.6** shows the schematic of the device used in the experiment. In this device, the number of pinholes on the working electrode in flow channel B was two and the diameter of the pinhole was 3 µm. A Ag/AgCl wire was placed on the left inlet of the flow channel A and connected to the working electrode terminal of the potentiostat. Another Ag/AgCl wire was placed on the KCl compartment of flow channel B and connected to the reference and counter electrode terminals of the potentiostat. The auxiliary flow channel used in the previous device was removed. To form the plug, air vents were formed on the left side and right side of the gold pattern in flow channel A.

4.2.9 Signal enhancement for protein detection by using redox cycling technique

Redox cycling technique was integrated to the coulometry coupled with metallization for investigating

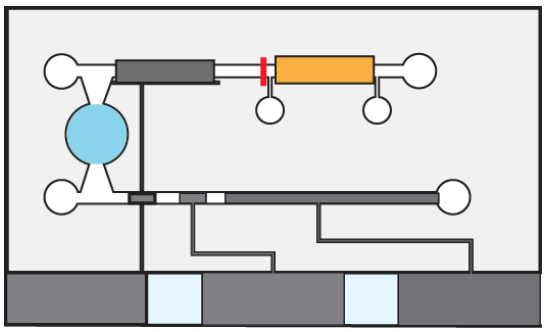

Figure 4.3. Device structure modification for plug measurement (1st modification). Rhombus structure for measuring the plug was removed.

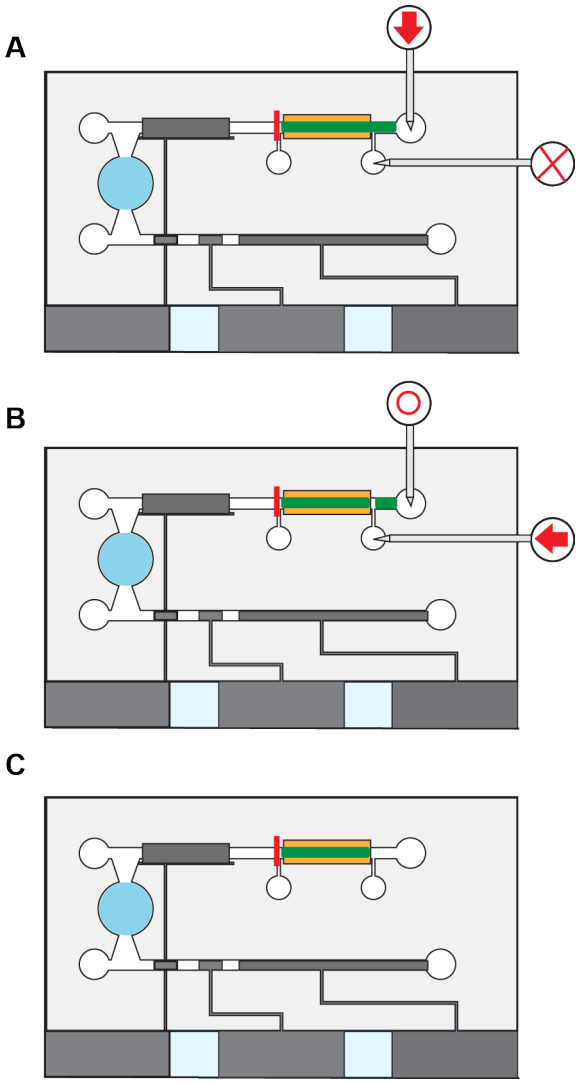

Figure 4.4. Procedure of plug processing on the new design of flow channel A. (A) Introduction of a solution into flow channel A. (B) Splitting of the solution using the air vent. (C) Incubation of the plug on the gold electrode.

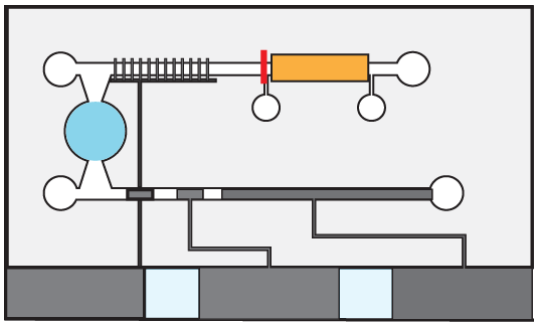

Figure 4.5. Modification of the working electrode in flow channel A (2nd modification). Structure of the platinum working electrode in flow channel A was changed into comb-like structure.

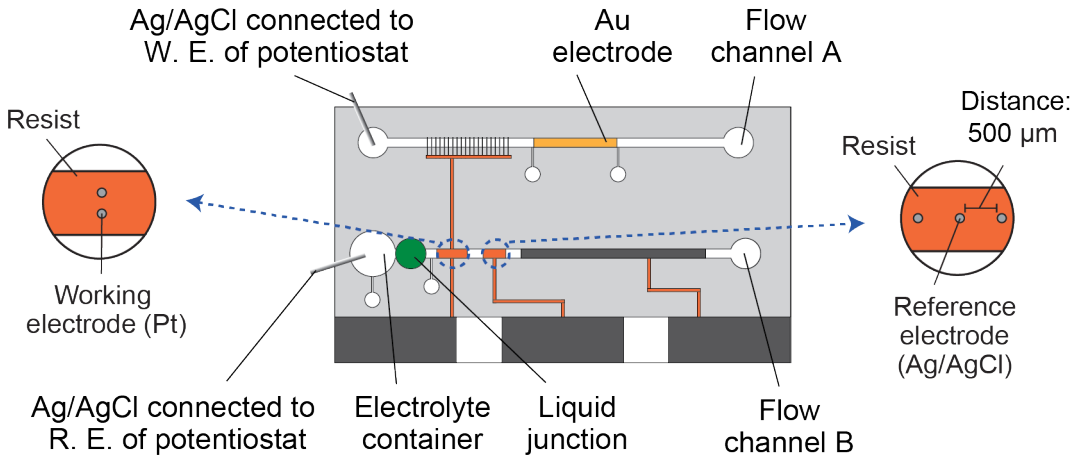

Figure 4.6. Schematic of the optimized device for protein detection.

the enhancement that could be obtained from such system. **Figure 4.7** shows the schematic of the device. The structure of the device was similar to that of the device shown in **Figure 4.6**. To make an array of interdigitated electrodes, an additional comb-like platinum electrode was formed in-between another comb-like platinum electrode in flow channel A (that connected to the working electrode in flow channel B). This electrode was used to apply the potential to the redox species solution that would be cycled. The amount of the analyte corresponded to the amount of the deposited silver on the working electrode in flow channel B. **Figure 4.8** shows the detection mechanism of this device. In the first part, the formation of the antigen-antibody complex on the gold electrode consisting of capture anti-AFP antibodies, AFP, and detection anti-AFP antibodies was conducted (**Figure 4.8**). Capture anti-AFP antibodies were immobilized by SAM of cysteine explained in **Section 2.2.4**. Detection anti-AFP antibodies were labeled with ALP enzyme that can produce PAP in the enzymatic reaction when the substrate solution of PAPP was introduced. PAP was oxidized on the platinum working electrode and generated *p*-quinone imine (QI). QI then redox cycled by applying a potential between working electrode 2 and the commercial reference electrode (**Figure 4.8**). During the oxidation of PAP, the silver ion in flow channel B would be reduced and deposited. This deposited silver was measured using coulometry.

For checking the performance of the device based on redox cycling, the detection of PAP was conducted. The procedure is shown in **Figure 4.9**. PAP solutions containing 0.1 M KCl was introduced in flow channel A and potential of 0.5 V was applied on working electrode 2 versus commercial reference electrode during redox cycling process

4.3 Results and discussion

4.3.1 Optimization of the BSA blocking

Optimization of the BSA was conducted through a simple fluorescence measurement. In this strategy, the amount of the adsorbed fluorescein particles on the PDMS wall reflecting the amount of the adsorbed GOD-antibody complexes which causing the non-negligible background. From the **Figure 4.9**, incubation time of 60 min of BSA was enough to obtain a small fluorescence intensity, in comparison to the background condition. Our previous selection of 30 min BSA incubation in **Section 2.2.4** was not enough for the blocking process. From this result, BSA incubation for 60 min was selected as a new parameter for the ELISA experiment in this chapter. A good blocking condition during the ELISA procedure can minimize the interference that comes from non-specific bonding/deposition of the biomolecules to the surface of gold.

4.3.2 Optimization of the plug volume

ELISA procedure from **Section 2.3.5** with BSA blocking of 60 min was selected. AFP concentration of 10 ng/mL and the background measurement were tested to see the performance of the device. **Figure 4.10** shows the result. By adjusting the plug volume to the size of the gold electrode, H_2O_2 produced from the ELISA

experiment was accumulated more effectively. As a result, the output charge from silver deposition was increased. The ratio of output charge and the background was improved from 3.8 to 4.9.

4.3.3 Optimization of the plug measurement method

ELISA described in **Section 2.3.5** was conducted to check the effect. Blocking by BSA was conducted for 60 min and AFP concentration of 10 ng/mL was selected to see the performance of the device. **Figure 4.11** shows the result. By removing the rhombus structure, the loss of the analyte could be reduced. The increase of the response charge indicates that more deposited silver was obtained. The ratio of output charge and the background was improved from 4.9 to 8.6.

4.3.4 Optimization of the working electrode in flow channel A

Reducing the area of the working electrode will reduce the background as similarly shown in the previous work (**Sassa et al., 2010**). ELISA explained in **Section 2.3.5** was conducted to check the effect. BSA blocking was conducted for 60 min and AFP concentration of 10 ng/mL was selected. **Figure 4.12** shows the reduction of the background when the shape of the electrode was change from rectangular shape (1st modification) to an array of strips (2nd modification). The background was reduced as the area of the working electrode area (or the sensing area) for the decomposition of H_2O_2 solution was reduced (**Sassa et al., 2010**). This H_2O_2 came from the non-specific binding of the protein. However, the charge for the detection of AFP was also reduced in this case. The ratio of output charge and the background was improved from 8.6 to 18.2.

4.3.5 Optimization of the working electrode in flow channel B

The working electrode structure in flow channel B was optimized to obtain the best reduced background while maintaining the similar amount of silver deposition. To reduce the background, similar strategy by reducing the area of the working electrode was adapted (**Sassa et al., 2010**). To check the effect of this changing, background charge measurement and detection of H_2O_2 were conducted (**Tsuchiya, 2017**). **Figure 4.13** shows the results of changing the area of the working electrode by changing the number of pinholes as the first approach. The effect of reducing the number of the pinholes working electrodes from 26 pinholes to 2 pinholes is the decreasing of the background charge of the device (**Figure 4.13A)**. The result agrees with the previous work (**Sassa et al., 2010**).

Next, the effect of reducing the number of microelectrodes was tested on the detection of H_2O_2 at three different concentrations; 10 µM, 1 µM, and 100 nM. The amount of deposited silver in high concentration (10 µM) of H_2O_2 was much reduced in the case of using 2 pinholes (**Figure 4.13B**). However, a clear advantage of using the smaller number of pinholes was shown when measuring the low concentration (100 nM) of H_2O_2 (**Figure 4.13D**). The ratio of the measured charge in a low concentration of H_2O_2 and the background charge

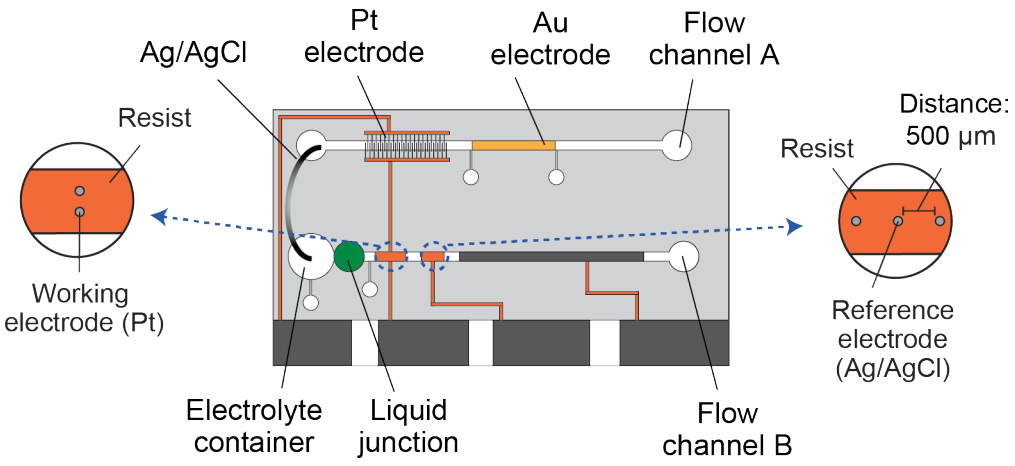

Figure 4.7. Schematic of the optimized device coupled with redox cycling for protein detection. Additional electrode was formed on the flow channel A.

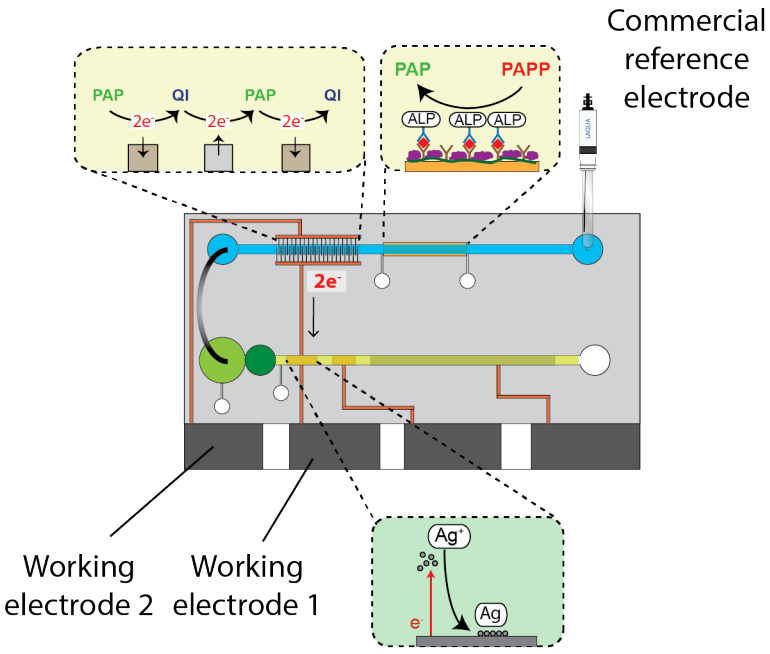

Figure 4.8. Principle of protein detection based on redox cycling technique using the device. (A) Formation of the antigen-antibody complex on the gold electrode. (B) Redox cycling process in flow channel A of the enzymatic reaction product generated from the ELISA procedure. Silver deposition was collected on the working electrode in flow channel B.

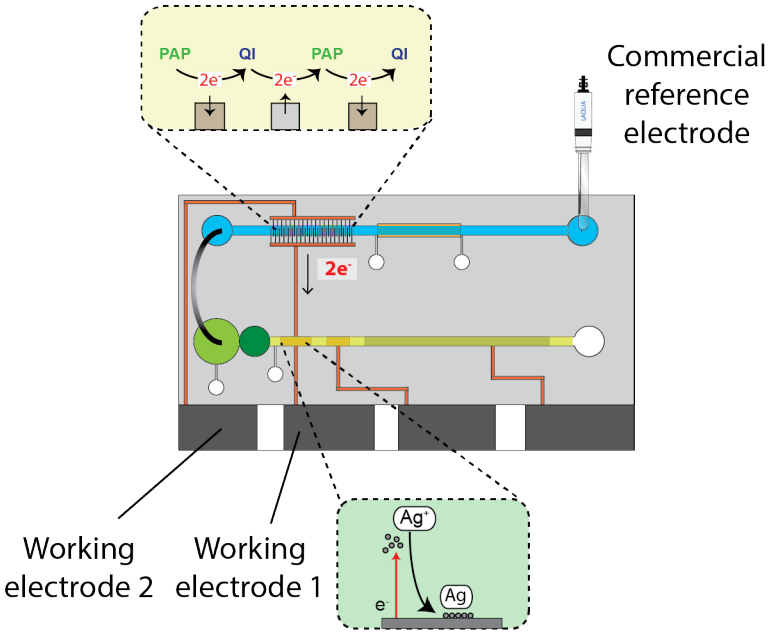

Figure 4.9. Procedure for detecting PAP sample.

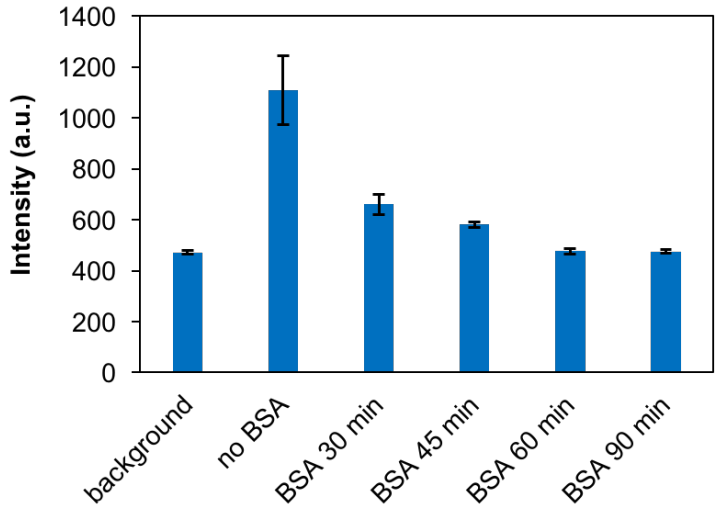

Figure 4.9. Change in fluorescence intensity on different blocking condition.

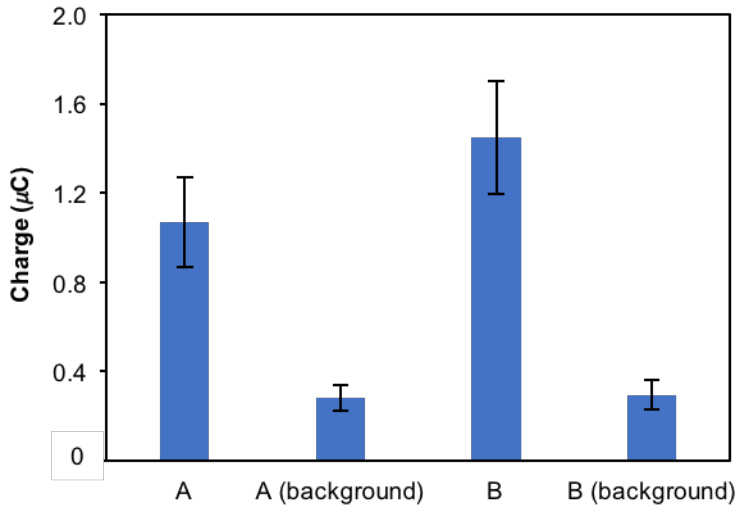

Figure 4.10. Change in coulometric responses after optimization of the plug volume. Data A was the output charge collected using glucose plug of 3.0 µL volume. Data B was the output charge collected using glucose plug of 1.5 µL. Background charges in both A and B conditions were shown.

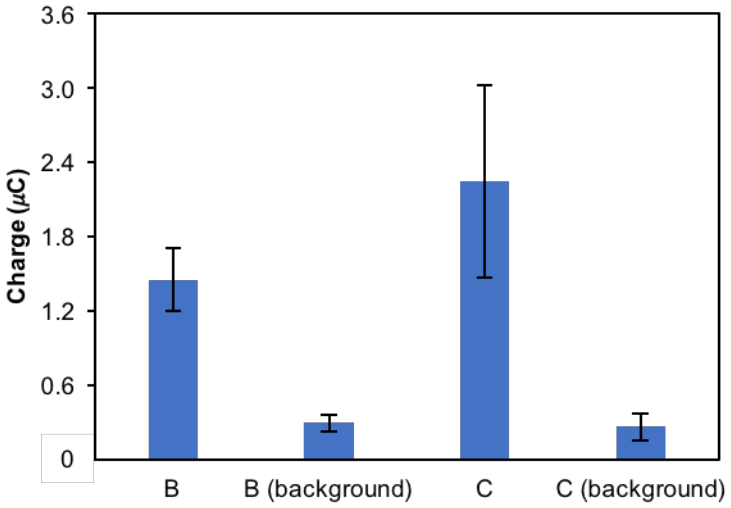

Figure 4.11. Change in coulometric response after structure modification of the device for plug measurement (data C). Data B was the previous result obtained when the plug volume was optimized. Data B was shown to compare the change of device performance.

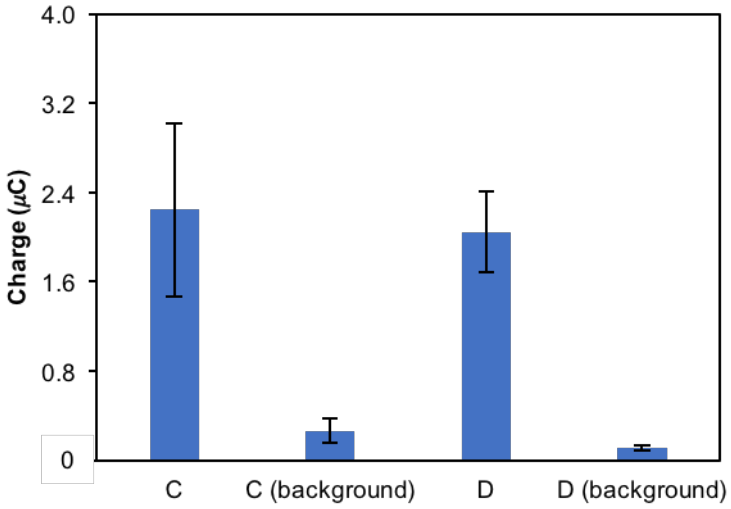

Figure 4.12. Change in coulometric response after modification of the working electrode structure in flow channel A (data D). Data C was the previous result obtained when the structure for measuring the plug was optimized. Data C was shown to compare the change of device performance.

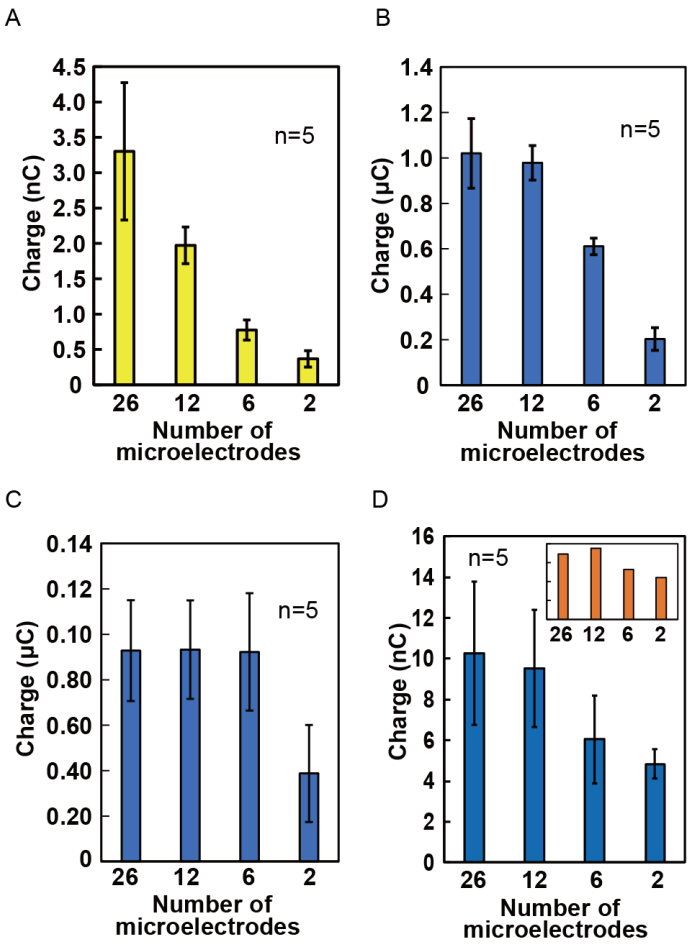

Figure 4.13. Effects of modification of the number of pinholes working electrode in flow channel B. (A) Changing of the background charge on different number of the microelectrodes. (B) Obtained charge when measuring 10 µM H_2O_2 on different number of the microelectrodes. (C) Obtained charge when measuring 1 µM H_2O_2 on different number of the microelectrodes. (D) Obtained charge when measuring 100 nM H_2O_2 on different number of the microelectrodes.

become larger when the number of pinholes is fewer. From this result, 2 pinholes were used as the optimized number of pinholes for working electrode.

On the second approach to reduce the background, the diameter of pinholes was reduced. **Figure 4.14** shows the results. When the diameter of the pinholes was reduced from 20 μm to 3 μm, the background charges become much reduced. Interestingly, when the measurement of H_2O_2 was conducted, the response charges were not much affected. From this result, 3 μm of the pinhole diameter was used as the optimized diameter of pinholes for working electrode.

4.3.6 Detection of AFP using the optimized parameters

After several optimizations of the parameters in ELISA and some changes in the device structure, detection of AFP was conducted. **Figure 4.6** shows the final figure of the device that combines all the optimized parameters. BSA blocking was conducted for 6o min. Metal junction was replaced with two metal wires (Ag/AgCl wires) connected to the potentiostat as an external voltage source (**Section 3.3.7, Figure 3.8**). Silver deposition was conducted by applying potential –0.6 V from the voltage source for 10 min. Detection procedure using the optimized device and parameters was listed in **Table 4.1**.

AFP concentrations from 1 ng/mL to 10 ng/mL were detected. Good linear relationship between AFP concentration and output charge was achieved (**Figure 4.15**). Limit of detection for AFP was 76.7 pg/mL (3σ). This result is five times higher than the one achieved using the device in **Chapter 2** (**Anshori et al., 2017**).

4.3.7 Signal enhancement for protein detection by using redox cycling technique

As a preliminary experiment, PAP was detected by redox cycling. A clear dependence of PAP concentrations and the output charges was shown (**Figure 4.16**). Detection limit was 80 pM. In a measurement of 1 μM PAP concentration, the output charge obtained using device based on redox cycling was 10 μC. However, in previous device (**Ikemoto et al., 2016**), measurement of 10 μM PAP concentration gave an output charge of only 1 μC. There was approximately an enhanced signal of 100 times in case of using redox cycling-based device. This technique shows a promising result for the detection of redox cycling substances in the research on electrochemical-based microdevice. Finally, detection of AFP using redox cycling technique was conducted. AFP concentrations from 0.1 ng/mL to 1 ng/mL were measured. 10 mM of PAPP was used as a substrate solution. **Table 4.2** shows the procedure of AFP detection. Detection limit of 19.6 pg/mL (3σ) was obtained. The detection limit was improved 4 times than that when using the metal wire connected with an external voltage source. From this study, redox cycling technique has been successfully integrated with the method of coulometry coupled with silver metallization.

4.4 Conclusions

Optimization of the device to achieve a highly sensitive detection of AFP have been conducted. BSA blocking process was optimized with 60 min incubation time is necessary for better blocking condition. Structure of the flow channel A was modified for the new plug measurement strategy where the previous auxiliary flow channel was removed to prevent the loss of analyte in the rhombuses structure. Modification of the working electrode in flow channel A and optimization of the pinholes working electrode in flow channel B have successfully reduced the background while keeping the performance of the device. Performance of the device for detecting the AFP using optimized device has improved to 76.7 pg/mL. Another enhancement technique using redox cycling shows more promising result. Device performance was increased four times and the detection limit has enhanced to 19.6 pg/mL. The work on the redox cycling method combined with system based on the coulometry coupled with silver metallization is interesting to be tested in diverse type of proteins analyte with different protein structure or size to see its performance.

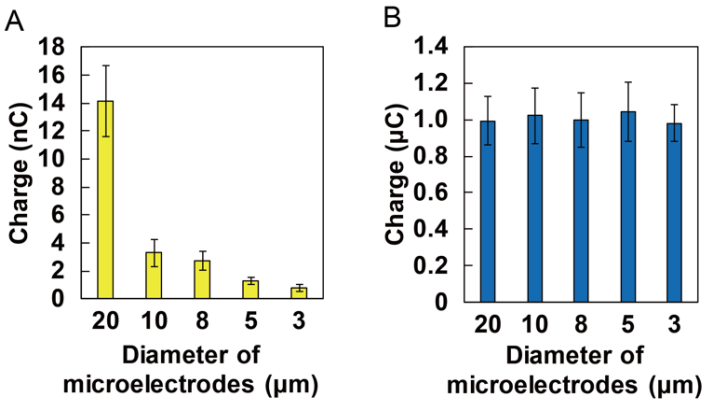

Figure 4.14. Effects of modifying the diameter of pinholes working electrode in flow channel B. (A) Changing of the background charge on different diameters of microelectrodes. (B) Dependence of the charge on the measurement of 10 μM H_2O_2 on different diameters of microelectrodes.

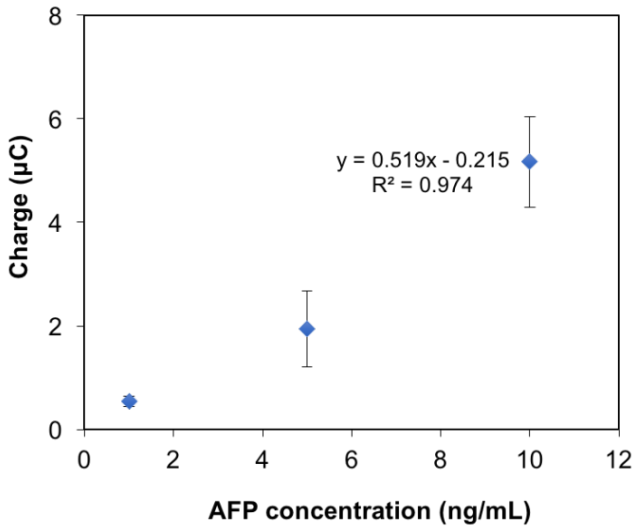

Figure 4.15. Dependence of output charge with the concentration of AFP using the optimized device.

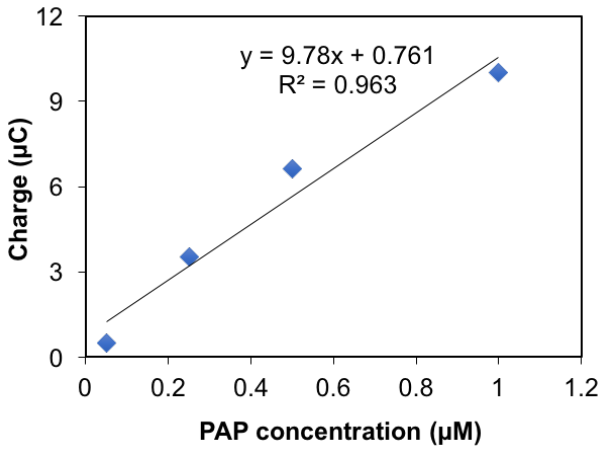

Figure 4.16. Dependence of output charge with the concentration of PAP using device based on redox cycling technique.

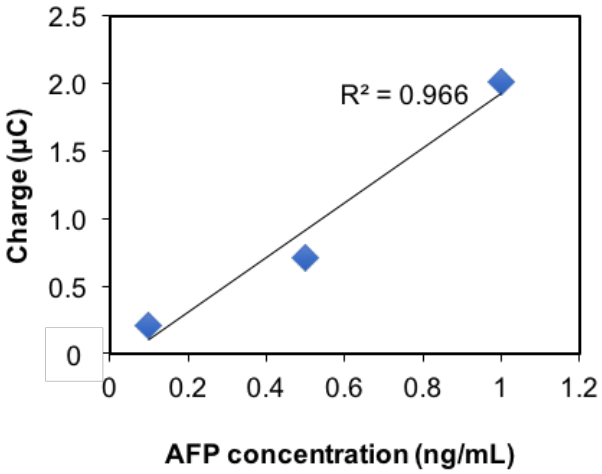

Figure 4.17. Dependence of output charge with the concentration of AFP using device based on redox cycling technique.

Table 4.1. Step of each procedure and its incubation time

Step	Incubation time (min)
1. AFP	30
2. Detection anti-AFP antibody labeled with GOD	30
3. Glucose introduction and H_2O_2 oxidation/silver deposition by applying –0.6 V	10

Table 4.2. Step of each procedure and its incubation time

Step	Incubation time (min)
1. AFP	30
2. Detection anti-AFP antibody labeled with GOD	30
3. PAPP introduction and H_2O_2 oxidation/silver deposition by applying 0.5 V on W. E. 2	10

Literature Cited

Ikemoto, K. et al. *Anal. Chem.,* **2016**, *88*, 9427-9434.

Anshori, I. et al. *Sens. Actuators. B*, **2018**, *256*, 835-838.

Sassa, F. et al. *Anal. Chem.*, **2010**, *82*, 8725-8732.

Tsuchiya, S. *Master Thesis,* Graduate School of Pure and Applied Sciences, University of Tsukuba, **2017**.

Chapter 5 Summary

In this dissertation, the development of a coulometric microfluidic device for highly sensitive detection of proteins is described.

Chapter 1 explains the current situation on infectious diseases as a major healthcare issue in developing countries. A brief history of the technological advances in MEMS and microfluidic techniques and POC devices were explained. Next, advantages of using electrochemical principles were mentioned, and the progress of the research on microfabricated coulometric devices was mentioned. Among them, our previous microfabricated coulometric device based on silver metallization was introduced. Based on these, the objectives of this study are mentioned.

Chapter 2 presented the microdevice for protein detection based on coulometry coupled with silver metallization. Immunoassay (ELISA) method was integrated on this device for the detection of target protein (AFP). The structure of the previous work was modified to include the location of ELISA in the device. The formation of antibody-antigen sandwich complexes on the gold pattern was possible through the formation of self-assembled monolayer (SAM). The optimization of the SAM of cysteine on the gold pattern to immobilize capture antibodies was conducted by fluorescent experiment. In the fluorescent experiment, an array of sputtered gold disks was formed on the glass substrate and stacked with PDMS substrate having a simple flow channel for introducing the SAM solutions. The amount of AFP was measured through the measurement of the amount of H_2O_2 produced from the enzymatic reaction of glucose oxidase (GOD) conjugated with the detection antibodies. Longer incubation was conducted to deposit more silver by replacing the used plug with a fresh one every 30 min. The limit of detection of AFP was 0.4 ng/mL with 120 min enzymatic reaction.

In **Chapter 3**, an idea was proposed for the enhancement of detection sensitivity of the electrochemical microdevice based on coulometry coupled with silver metallization. By using a metal wire to connect two flow channels as an alternative to a liquid junction, the potentials for the oxidation of the analyte and deposition of silver could be shifted separately. Three methods were proposed in this study. First method is to use a silver wire with Ag/AgCl electrodes formed at the ends to connect the two flow channels. By changing KCl concentration in flow channel A while keeping the electrolyte concentration in KCl the same, the potentials of the platinum electrodes could be shifted to values that are more positive and negative than that of the mixed potential, respectively. However, with this approach, the potential difference on both ends of the wire could not be large sufficiently (<100 mV), thus limiting the enhancement. The second method is to change one side of the metal wire with zinc or nickel to achieve a larger electrode potentials difference to enhance the oxidation and reduction reactions on the platinum electrodes. In the third method, a potential difference was applied through two Ag/AgCl wires using an external voltage source. The sensitivity of the device increased as the potential difference increased. With this technique, the detection limit for H_2O_2 was 2.4 nM. This value is ten times lower than that of the previous device (**Ikemoto et al., 2016**).

Chapter 4 presented some strategies to improve the performance of the coulometric microdevice for protein detection. First improvement was the blocking process optimization using BSA. Fluorescence intensity was measured with different BSA incubation times and the result was compared with that of the background. 60 min BSA incubation was the optimized parameter. Second, the plug volume was reduced to accumulate the enzymatic reaction product effectively. Third, flow channel structure to measure the plug volume was modified. Fourth, the shape of the working electrode in flow channel A was changed from a rectangle to a comb-like shape. Each of these improvements resulted in the increase of the output charge / background ratio. Fifth, the structure of the working electrode in flow channel B was optimized by changing the number and diameter of the pinholes in the electrode structure. Based on the result of characterization, 2 pinholes of 3 μm in diameter were used for the working electrode. Detection of AFP was tested under these optimized conditions by applying potential from external voltage source. The detection limit of AFP was 76.7 pg/mL (3σ). Finally, signal enhancement by redox cycling was tried. An additional electrode was formed in the sensing area of flow channel A to form an interdigitated electrode array. Alkaline phosphatase was used as the enzyme label to produce p-aminophenol (PAP). PAP is product of the enzymatic reaction that can be redox cycled. When PAP was detected by redox cycling, a detection limit of 80 pM was achieved. Next, AFP was detected. In this case, the detection limit was 19.6 pg/mL (3σ). The detection limit was improved 4 times than that when using two metal wires connected to the external voltage source.

In the studies presented here, a clear direction to realize a portable device for protein detection was demonstrated. Although excellent performance has already been demonstrated, there are still some points to be considered for further improvement of performance and development of more advanced devices. For example, the metal wire connection will be a powerful technique to realize novel devices for multiplex detection that may be used for POCT.

Appendix

Information of reagents, materials, equipment used for the fabrication, trial and evaluation of devices as well as experiments mentioned in chapter 2 to chapter 4 are summarized below.

Reagents and materials

- Glass substrate: (wafer of 3-inch diameter) Pyrex glass material, 76.2 × 0.5 μm, Corning Japan.
- Positive photoresist: Microposit, S1818, Shipley.
- For a positive resist developing solution: Microposit developer, MF319, Shipley.
- For a thick film negative photoresist: SU-8, Microchem.
- SU-8 for the developer: SU-8 developer, Microchem.
- PDMS (Polydimethylsiloxane) precursor: KE-1300T, ShinEtsu.
- PDMS curing agent: CAT-1300, ShinEtsu.
- Dry film photoresist: A5312-02-B02, Mitsubishi paper mills ltd., Osaka, Japan.
- Potassium chloride: KCl, Wako Pure Chemistry.
- 25% ammonia water: NH_4OH, Wako Pure Chemistry.
- 30% hydrogen peroxide: H_2O_2, Wako Pure Chemistry.
- Acetone: C_3H_6O, Wako Pure Chemistry.
- Toluene: $C_6H_5CH_3$, Wako Pure Chemistry.
- 2-propanol: C_3H_8O, Wako Pure Chemistry.
- Sulfuric acid: H_2SO_4, Wako Pure Chemistry.
- Hydrochloride: HCl, Wako Pure Chemistry.
- Zinc chloride: $ZnCl_2$, Wako Pure Chemistry.
- Ammonium chloride: NH_4Cl_2, Wako Pure Chemistry.
- Nickel (II) sulfate hexahydrate: $NiSO_4.6H_2O$, Wako Pure Chemistry.
- Nickel (II) chloride hexahydrate: $NiCl.6H_2O$, Wako Pure Chemistry.
- Trisodium citrate dehydrate: $C_6H_5Na_3O_7.2H_2O$, Wako Pure Chemistry.
- Silver nitrate: $AgNO_3$, Wako Pure Chemistry.
- Potassium nitrate: KNO_3, Wako Pure Chemistry.
- Sodium hydroxide: NaOH, Wako Pure Chemistry.
- Bovine serum albumin (BSA): Wako Pure Chemistry.
- Fluorescein: Wako Pure Chemistry.
- Low temperature agarose powder: Agarose-L, Wako Pure Chemical Industries.
- Detection anti-AFP antibody: Polyclonal rabbit anti-human alpha-1-fetoprotein antibody (H-140), Santa Cruz Biotechnology, USA.
- AFP antigen: Human alpha-1-fetoprotein standard, Dako, Japan.

- Capture anti-AFP antibody: Polyclonal goat anti-human alpha-1-fetoprotein antibody (C-19), Santa Cruz Biotechnology, USA.
- L-cysteine: Dojindo Chemical, Japan.
- Water soluble carbodiimide: WSC, Wako Pure Chemical Industries.
- *N*-Hydroxysuccinimide: NHS, Wako Pure Chemical Industries.
- Bovine serum albumin: BSA, Wako Pure Chemical Industries.
- Glucose oxidase: GOD, Wako Pure Chemical Industries.
- D-Glucose: Wako Pure Chemical Industries.
- Silver wire: 0.5 mm (diameter), The Nilaco Corp.
- PVA-SbQ, SPP-H13: Toyo Gosei, Japan.
- Alkaline phosphatase (ALP) conjugation kit: Dojindo Chemical, Japan.
- 4-aminophenylphosphate monosodium salt hydrate (PAPP): Enzo Life Sciences, USA.

Equipment

- ✓ Sputter deposition equipment: CFS-4ES-231, Shibaura Eletec.
- ✓ Spin coater: 1H-D7, Mikasa.
- ✓ Mask aligner: MA-10, Mikasa.
- ✓ Dicing equipment: A-WD-10A, Tokyo seimitsu.
- ✓ Dry oven: OF-450, AS ONE.
- ✓ Hot plate: ND-1, AsOne.
- ✓ Basic plasma kit: BP-1, Samco.
- ✓ Pure water manufacturing equipment: DirectQ 3 UV with pump, Millipore.
- ✓ Potentiostat/galvanostat: HA-151, Hokuto denko.
- ✓ Potentiostat/galvanostat: PGSTAT12, Autolab, Eco Chemie.
- ✓ UV irradiation device: ENF-280C / J, Spectronics.
- ✓ Thermostatic bath: WBS-80A, AS ONE.
- ✓ PH meter: Seven compact S220, METTLER TOLEDO.
- ✓ Microscope: SMZ1500, Nikon.
- ✓ CCD camera: DCR-SX41, Sony.
- ✓ Digital cameras: NEX-5N, Sony.
- ✓ Laser microscope: VK-8510, Keyence, Osaka, Japan.
- ✓ Entity fluorescence microscope system: VB-G25, Keyence.
- ✓ Excitation filter: XF1067, Omega Optical.
- ✓ Fluorescent filter: XF3081, Omega Optical.
- ✓ Fluorescence microscope: IX-73, Olympus, Japan.
- ✓ Filter unit: Cy5−4040C, Olympus, Japan.
- ✓ CMOS camera: ORCA-Flash 4.0, Hamamatsu Photonics, Japan.

- ✓ Silver / silver chloride reference electrode: # 2080A-06T, HORIBA.
- ✓ Punch: Punch no. 1256, Takashiba Gimune Seisakujo, Hyogo, Japan
- ✓ Biopsy punch: Kai industries, Gifu pref., Japan.
- ✓ Mask drawing software: Adobe Photoshop CS6, Autocad 2016.

Fabrication of the electrode chip

Glass substrate cleaning

Boil the washing solution (25% NH_3 : 30% H_2O_2 : deionized water = 1 : 1 : 4). Immerse the glass substrate in the washing solution for 5 min and boiled deionized water for 5 min (repeat one more time). Dry the glass substrate using the nitrogen gas.

Patterning Pt/Cr lift-off resist

Spin coat positive photoresist (S1818G) (500 rpm, 5 s → 2000 rpm, 10 s) on the glass substrate surface. Bake the glass substrate in the 80 °C dry oven for 30 min. Form the Pt/Cr lift-off pattern on the glass substrate by placing the printed designed mask and exposing it to ultra violet light emitted from the mask aligner for 70 s. After that, immerse the glass substrate in toluene (30 °C) for 30 s and bake it in the 80 °C dry oven for 15 min. Develop the exposed positive photoresist film on the glass substrate in the positive photoresist developer for 1 min, rinse with deionized water and dry with N_2 gas.

Pt/Cr sputtering

Dry etch the glass substrate at 200 W (5 min). Sputter the Cr layer (5 min) and the Pt layer (15 min × 2) on the glass substrate by the sputtering machine. The output power was maintained at 100 W during the sputtering process.

Pt/Cr lift-off

Immerse the sputtered glass substrate in acetone for 1 h. Next, slowly peel the Pt/Cr layer which does not cover the electrode region from the glass substrate. Wash the glass substrate again with acetone and dry with N_2 gas.

Patterning Au/Cr lift-off resist

Spin coat positive photoresist (S1818G) (500 rpm, 5 s → 2000 rpm, 10 s) on the glass substrate surface. Bake the glass substrate in the 80 °C dry oven for 30 min. Form the Au/Cr lift-off pattern on the glass substrate by placing the printed designed mask and exposing it to ultra violet light emitted from the mask aligner for 70 s. After that, immerse the glass substrate in toluene (30 °C) for 30 s and bake it in the 80 °C dry oven for 15

min. Develop the exposed positive photoresist film on the glass substrate in the positive photoresist developer for 1 min, rinse with deionized water and dry with N_2 gas.

Au/Cr sputtering

Dry etch the glass substrate at 200 W (5 min). Sputter the Cr layer (5 min) and Au layer (15 min × 2) on the glass substrate by the sputtering machine. The output power was maintained at 100 W during the sputtering process.

Au/Cr lift-off

Immerse the sputtered glass substrate in acetone for 1 h. Next, slowly peel the Au/Cr layer which does not cover the electrode region from the glass substrate. Wash the glass substrate again with acetone and dry with N_2 gas.

Patterning Ag lift-off resist

Spin coat positive photoresist (S1818G) (500 rpm, 5 s → 2000 rpm, 10 s) on the glass substrate surface. Bake the glass substrate in the 80 °C dry oven for 30 min. Form the Ag lift-off pattern on the glass substrate by placing the printed designed mask and exposing it to ultra violet light emitted from the mask aligner for 70 s. After that, immerse the glass substrate in toluene (30 °C) for 30 s and bake it in the 80 °C dry oven for 15 min. Develop the exposed positive photoresist film on the glass substrate in the positive photoresist developer for 1 min, rinse with deionized water and dry with N_2 gas.

Ag sputtering

Sputter the Ag layer (15 min × 2) on the glass substrate by sputtering machine. The output power was maintained at 100 W during the sputtering process.

Ag lift-off

Immerse the sputtered glass substrate in the acetone for 1 h. Next, slowly peel the Ag layer which does not cover the electrode region from the glass substrate. Wash the glass substrate again with acetone and dry with N_2 gas.

Patterning insulation layer

Spin coat positive photoresist (S1818G) (500 rpm, 5 s → 2000 rpm, 10 s) on the glass substrate surface. Bake the glass substrate in the 80 °C dry oven for 30 min. Form the Ag lift-off pattern on the glass substrate by placing the printed designed mask and exposing it to ultra violet light emitted from the mask aligner for 70 s.

Dicing

Immobilize the glass substrate on the immobilization sheet. Cut the glass substrate into devices one by one and rinsed it with by deionized water. Develop the exposed positive photoresist film on a diced glass substrate in the positive photoresist developer for 1 min, rinse with deionized water and dry with N_2 gas. Post bake the device in the 120 ^oC dry oven for 30 min. The size of one chip was 30 mm × 22 mm.

Forming Ag/AgCl layer

The Ag electrode on the device, the commercial Ag/AgCl electrode and the platinum plate are regarded as working electrode, reference electrode and auxiliary electrode, respectively. Immerse the above three electrodes 0.1 M KCl in a glass beaker with a magnetic stirrer is turned on. Connect them to the autolab and apply a 50 nA current to the electrodes for 15 min by autolab. Wash the device with deionized water and dry with N_2 gas

Fabrication of PDMS substrate

Glass substrate cleaning

Boil the washing solution (25% NH_4OH : 30% H_2O_2 : deionized water = 1 : 1 : 4). Immerse the glass substrate in the washing solution for 5 min and boiled deionized water for 5 min (repeat one more time). Dry the glass substrate using the nitrogen gas.

Formation of SU-8 pattern (lower part)

Dry etch the glass substrate with O_2 plasma for 1 min. The output power was 100 W. Spin coat SU-8 (500 rpm, 5 s → slope, 10 s → 800 rpm, 15 s) onto the glass substrate and pre-bake the glass substrate on the hot plate at 65 °C and 95 °C for 5 min and 25 min, respectively. Form the SU-8 pattern (lower part) on the glass substrate by placing the printed designed mask and exposing it to ultra violet light emitted from the mask aligner for 180 s. After exposure, post-bake the glass substrate on the hot plate at 65 °C for 10 min.

Development of SU-8 (lower part)

Develop and rinse SU-8 in the SU-8 developer. In addition, wash the glass substrate in 2-propanol to clean it from contamination. Dry the glass substrate with N_2 gas.

Formation of SU-8 pattern (higher part)

Dry etch the glass substrate with O_2 plasma for 3 min. The output power was 100 W. Spin coat SU-8 (500 rpm, 5 s → 2000 rpm, 15 s) onto the glass substrate. Additionally, put a more 3 g SU-8 on the glass substrate.

Then, pre-bake the glass substrate on the hot plate at 65 °C and 95 °C for 10 min and 8 h, respectively. Form the SU-8 pattern (higher part) on the glass substrate by placing the printed designed mask and exposing it to ultra violet light emitted from the mask aligner for 600 s. Post-bake the glass substrate on the hot plate at 65 °C for 20 min.

Development of SU-8 (higher part)

Develop and rinse SU-8 in the SU-8 developer. In addition, wash the glass substrate in 2-propanol to clean it from contamination. Dry the glass substrate with N_2 gas. The SU-8 template has been completed.

Preparation and coating of PDMS

Mix the precursor solution of PDMS and curing solution with a mass ratio of 10 : 1. Coat the mixture on the SU-8 template uniformly and get rid of air bubbles by a vacuum pump. After that, cure the PDMS in the 80 °C dry oven for 30 min and peel it from SU-8 template. Cut the PDMS into flow channels one by one

List of publications

Publication

Isa Anshori and Hiroaki Suzuki, "Microfluidic Device for High-Sensitivity Coulometric Detection of Proteins", *Sensors and Actuators B: Chemical* (**2017**).

International conference proceeding

Isa Anshori and Hiroaki Suzuki, "Electrochemical Microdevices for Proteins Based on Coulometry Coupled with Silver Metallization", *19th International Conference on Solid-State Sensors, Actuators and Microsystems (TRANSDUCERS), IEEE* **2017**.

Isa Anshori and Hiroaki Suzuki, "Microdevice for Coulometric Determination of Proteins Coupled with Metallization", *Asia-Pacific Conference of Transducers and Micro-Nano Technology (APCOT)* **2016**.

Local conference proceedings

Isa Anshori and Hiroaki Suzuki, "Highly sensitive detection of proteins by coulometry coupled with silver metallization", *IEEJ Technical Meeting on Sensors and Micromachines* **2015**.

List of conferences

Isa Anshori and Hiroaki Suzuki, "Electrochemical Microdevices for Proteins Based on Coulometry Coupled with Silver Metallization", the 19th International Conference on Solid-State Sensors, Actuators and Microsystems (Transducers 2017), IEEE, Kaohsiung, Taiwan, June 2017.

Isa Anshori and Hiroaki Suzuki, "Electrochemical Microdevices for Proteins Based on Coulometry Coupled with Silver Metallization", IEEJ Spring Meeting 2017, Toyama, Japan, March 2017.

Isa Anshori, Masatoshi Yokokawa, and Hiroaki Suzuki, "Microdevice for Coulometric Detection of α-Fetoprotein Coupled with Metallization Microdevice for Coulometric Detection of α-Fetoprotein Coupled with Metallization", 6th Anniversary-Interdisciplinary Workshop on Science and Patents (IWP) 2016, Tsukuba, Japan, September 2016.

Isa Anshori and Hiroaki Suzuki, "Electrochemical Microdevices for Proteins Based on Coulometry Coupled with Silver Metallization", Asia-Pacific Conference of Transducers and Micro-Nano Technology (APCOT) Kanazawa, Japan, June 2016.

Isa Anshori, Masatoshi Yokokawa, and Hiroaki Suzuki, "Highly sensitive electrochemical immunoassay by coulometry coupled with silver metallization Highly sensitive electrochemical immunoassay by coulometry coupled with silver metallization", 5th Anniversary-Interdisciplinary Workshop on Science and Patents (IWP) 2015, Tsukuba, Japan, September 2015.

Isa Anshori and Hiroaki Suzuki, "Highly sensitive detection of proteins by coulometry coupled with silver metallization", IEEJ Technical Meeting on Sensors and Micromachines 2015, Kyushu, Japan, July 2015.

Acknowledgements

I would first like to thank my research advisor, Prof. Hiroaki Suzuki. Without his continued guidance and support none of the research in this dissertation would have been possible. I have benefited immensely, both scientifically and personally, from my time under his mentorship. I would also like to thank Prof. Masatoshi Yokokawa and Prof. Edwin T. Carlen for providing me constructive comments and suggestions to refine my works. I am also grateful to the Japanese government for the financial support as MEXT scholarship for continuing my higher study at Japan.

Science is becoming far more interconnected, and the research in this dissertation is no exception. Without the help of my coauthors and colleagues, this research would not have been realized. Special thanks must go to my colleagues in the Suzuki-Yokokawa research group, for valuable education, discussion: Ken Uchiyamada, Shuichi Takie, Shinnosuke Tsuchiya, Koki Kariya, Miah Md Abunasar, Mohosin Rana and Shishir Kanthi Pramanik. I would like to thank all the lab members, former and present, for all the supports and discussions during my doctoral program. I really appreciate it very much. I would also like to thank my friends, and colleagues at the University of Tsukuba for their encouragement and moral support which made my stay and studies in Tsukuba more enjoyable.

I am very thankful and fortunate enough to get constant support and full encouragement to always enjoy the study and the research life from my lovely wife, my lovely mom and my lovely families. I love you all. At last, to my dad in heaven who passed away because of cancer, I would like to say, “This work is for you. Have a happy life there.”